Carnegie Mellon

Textures in Thermomechanical Processing (TMP) of Metals

A. D. Rollett

27-750

Texture, Microstructure & Anisotropy

Last revised: 26th Apr. 2016

MSE

Objectives

- Introduce you to experimentally observed textures in a wide range of materials.
- Develop a taxonomy of textures based on deformation type.
- Prepare you for relating observed textures to theoretical (numerical) models of texture development, especially the *Taylor* model.
- See chapter 5 in Kocks, Tomé & Wenk.
- Some slides courtesy of Prof. P. Kalu (FAMU) and Prof. D. Waryoba (Penn State Dubois)

Taxonomy

- Note that *solidification* often introduces texture where the microstructure is columnar because it is usually dendritic and the preferred growth direction is <100>. Equi-axed microstructures are nearly random.
- Deformation history more significant than alloy.
- Crystal structure determines texture through slip (and twinning) characteristics.
- Alloy (and temperature) can affect textures through planarity of slip.
- Annealing (recrystallization) sometimes produces a drastic change in texture, especially in pure fcc metals.

Why does deformation result in texture development?

- Qualitative discussion:
- Deformation means that a body changes its shape, which is quantified by the plastic strain, ε_p.
- Plastic strain is accommodated in crystalline materials by dislocation motion, or by re-alignment of long chain molecules in polymers.

Dislocation glide ⇒ grain reorientation

- Dislocation motion at low (homologous) temperatures occurs by glide of loops on crystallographic planes in crystallographic directions: *restricted glide*.
- Restricted glide throughout the volume is equivalent to uniform shear.
- In general, shear requires lattice rotation in order to maintain grain alignment: *compatibility* is required, which is the basis for the Taylor model.

Re-orientation → Preferred orientation

- Reorientations experienced by grains depend on the type of strain (compression versus rolling, e.g.) and the type of slip (e.g. {111}<110> in fcc).
- In general, some orientations are unstable (*f(g)* decreases) and some are stable (*f(g)* increases) with respect to the deformation imposed, hence *texture development*.

The Taylor model

- The *Taylor* model has one basic assumption: the change in shape (micro-strain) of each grain is identical to the body's change in shape (macro-strain).
- Named for G.I. Taylor, English physicist, mid-20th century; first to provide a quantitative explanation of texture development.

The Taylor model

- The *Taylor* model has one basic assumption: the change in shape (micro-strain) of each grain is identical to the body's change in shape (macro-strain).
- Named for G.I. Taylor, English physicist, mid-20th century; first to provide a quantitative explanation of texture development.
- This was discussed in the lecture on multiple slip (L11).

Taylor G (1938) "Plastic strain in metals", *J. Inst. Metals* (U.K.) **62** 307

Single slip models ineffective

- Elementary approach to single crystal deformation emphasizes slip on a single deformation system.
- Polycrystal texture development requires *multiple slip systems* (5 or more, as dictated by von Mises).
- *Cannot use simple rules*, e.g., alignment of slip plane with compression plane!

Deformation systems (typical)

- Fcc metals (low temperature): {111}<110>
- Bcc metals: {110}<111>, {112}<111>, {123}<111>, pencil glide

Hexagonal metals:
{1010}<1210>; prismatic
{0001}<1210>; basal
{1012}<1011>$_{twin}$;
{1011}<1123>; pyramidal, or c+a
{2112}<2113>$_{twin}$.

TOMÉ *et al.*: MECHANICAL RESPONSE OF Zr. Part I

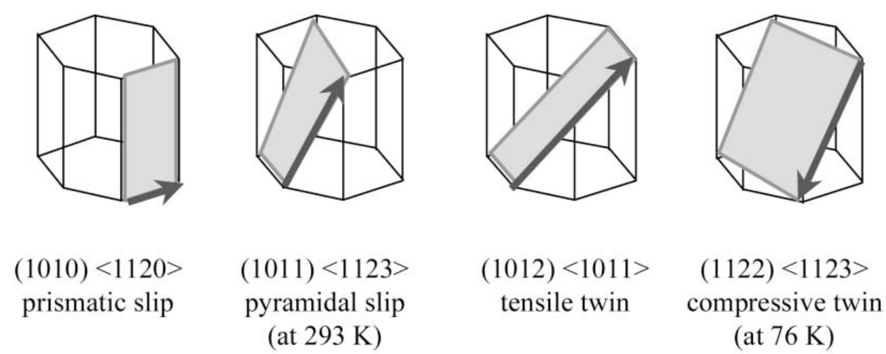

4. Active deformation systems in Zr considered in this work: prismatic slip, tensile twinning and py slip at 293K; prismatic slip, tensile twinning and compressive twinning at 76K.

Deformation systems (typical)

Material Class	**Primary System**	**Secondary Systems**
Face-centered cubic metals	$\{111\}\langle 1\bar{1}0\rangle$	
Body-centered cubic metals	$\{110\}\langle \bar{1}11\rangle$	$\{123\}\langle 11\bar{1}\rangle$ $\{112\}\langle 11\bar{1}\rangle$
Hexagonal close-packed metals (c/a>1.633) (e.g. Be, Cd, Zn and Mg)	$\{0001\}\langle 11\bar{2}0\rangle$	$\{11\bar{2}2\}\langle 11\bar{2}3\rangle$ $\{10\bar{1}1\}\langle 11\bar{2}0\rangle$
Hexagonal close-packed metals (c/a<1.633) (e.g. Zr,Ti and Hf)	$\{10\bar{1}0\}\langle 11\bar{2}0\rangle$	$\{11\bar{2}2\}\langle 11\bar{2}3\rangle$ $\{10\bar{1}1\}\langle 11\bar{2}0\rangle$
Diamond cubic (fcc) (e.g. Si, Ge and diamond)	$\{111\}\langle 1\bar{1}0\rangle$	
Rock Salt (fcc) (e.g. MgO, LiF, NaCl)	$\{110\}\langle 1\bar{1}0\rangle$	
CsCl (simple cubic)	$\{110\}\langle 001\rangle$	
Al2O3 (hexagonal)	$\{0001\}\langle 11\bar{2}0\rangle$	$\{11\bar{2}0\}\langle 1\bar{1}01\rangle$ $\{1\bar{1}02\}\langle 1\bar{1}01\rangle$
BeO (hexagonal)	$\{0001\}\langle 11\bar{2}0\rangle$	$\{10\bar{1}0\}\langle 11\bar{2}0\rangle$ $\{10\bar{1}0\}\langle 0001\rangle$

In deformed materials, texture or preferred orientation exists due to the anisotropy of slip. While slip in bcc metals generally occurs in the <111> type direction, it may be restricted to {110} planes or it may involve other planes. In general, texture development in bcc metals appears to involve <111>{112} as well as <111>{110}, but this may reflect easy cross-slip between different {110} planes, not actual {112} slip planes.

(*T. H. Courtney, Mechanical Behavior of Materials, McGraw-Hill, New York, 1990.*)

Strain Measures

- Strain commonly defined as a scalar measure of (plastic, irreversible) deformation: logarithmic strain:=

$$\varepsilon = \ln \{l_{new}/l_{old}\}$$

- Rolling strain: typical: reduction in thickness:= $r = 100\% \text{ x } h_{new}/h_{old}$
better to use *von Mises equivalent strain*:

$$\varepsilon_{vM} = 2/\sqrt{3} \ln \{l_{old}/l_{new}\}$$

Deformation Modes: sample symmetry

- Tension, Wire Drawing, Extrusion C_∞
- Compression, Upsetting C_∞
- Torsion, Shear 2
- Plane Strain Compression, Rolling mmm
- Deformation modes of uniaxial type generate fiber textures, i.e. a single common crystal axis parallel to the deformation axis
- Shear gives monoclinic symmetry
- Plane strain gives orthorhombic symmetry

Axisymmetric deformation: Extrusion, Drawing

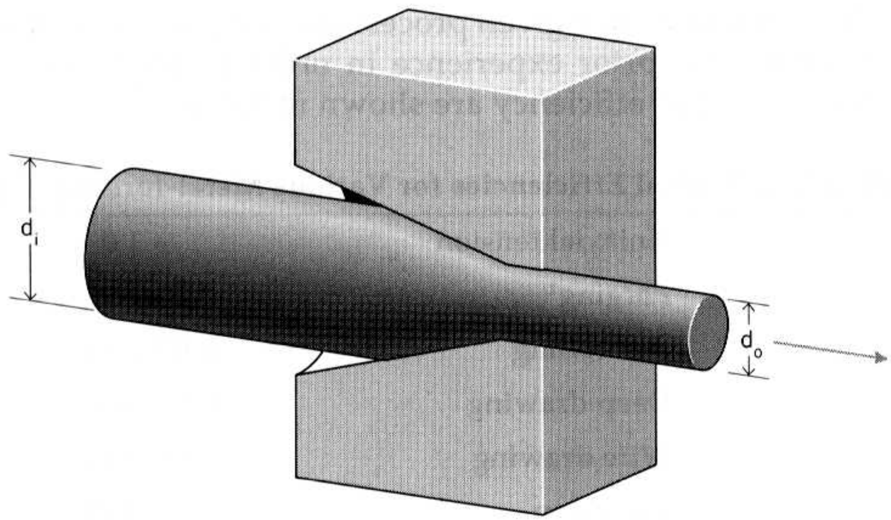

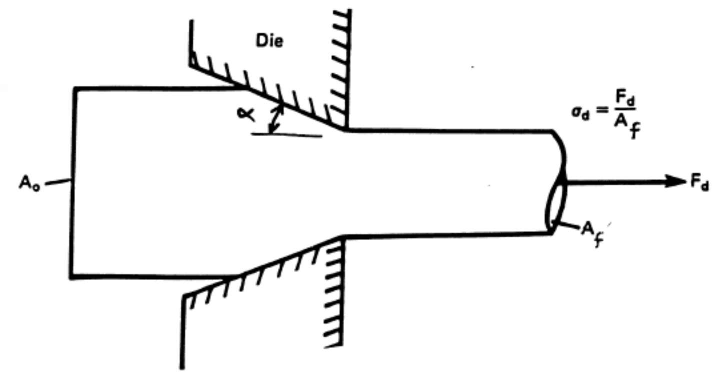

α is the "die angle"; smaller angles give more uniform deformation but higher friction forces

$$\varepsilon = \begin{pmatrix} +\Delta & 0 & 0 \\ 0 & -0.5\Delta & 0 \\ 0 & 0 & -0.5\Delta \end{pmatrix}$$

Uniaxial Strain

$$d\varepsilon = \begin{pmatrix} +\Delta & 0 & 0 \\ 0 & -\Delta/2 & 0 \\ 0 & 0 & -\Delta/2 \end{pmatrix}$$

Inverse Pole Figures (FCC)

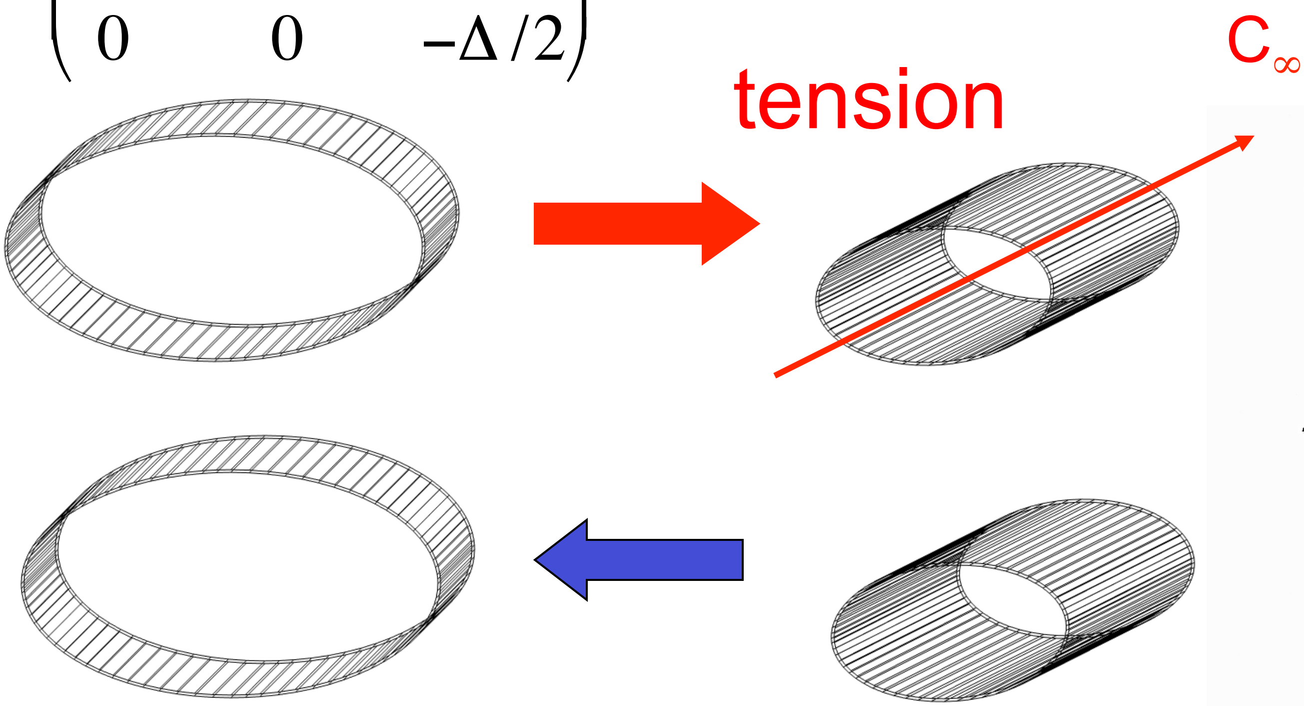

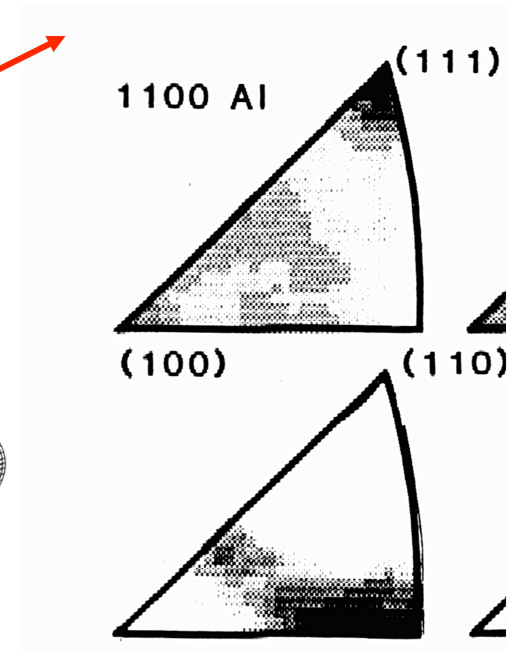

compression

$$d\varepsilon = \begin{pmatrix} -\Delta & 0 & 0 \\ 0 & +\Delta/2 & 0 \\ 0 & 0 & +\Delta/2 \end{pmatrix}$$

See Ch. 5 in Kocks, Tomé & Wenk

Uniaxial Modes - C_∞

Deformation mode/	fcc/	bcc/	hcp (Ti)
Wire drawing, Round extrusion.	<111> & <100>	<110>	<10-10>
Upsetting, Uniaxial compression.	<110>	<111> &<100>	<0001>

Note exchange of types between *fcc* & *bcc*

Axisymmetric deformation

- In fcc metals, axisymmetric deformation (e.g. wire drawing) produces fiber texture: <111> + <100> duplex, parallel to the wire.

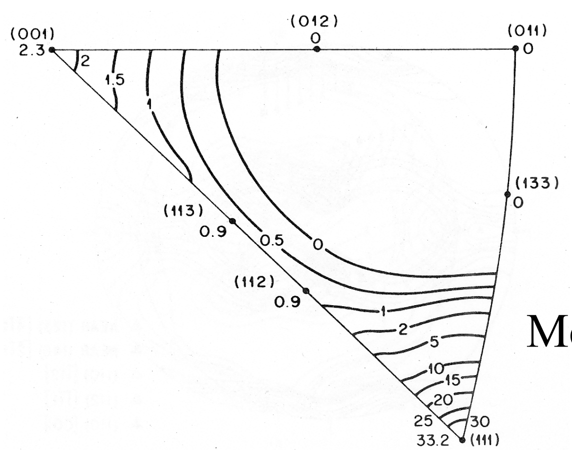

McHargue et al., 1959

Schmid and Wassermann (1963): 60% <111> + 40% <100>

Ahlborn and Wassermann (1963): 66% <111> + 34% <100>

} Electrolytic Copper

Axisymmetric deformation

- Axisymmetric deformation ~ higher order symmetry, C_∞
- Texture can be represented by an *inverse pole figure* (IPF).
- In IPF, contour lines show the frequency with which the various directions, <uvw>, in the crystal coincide with the specimen axis under consideration

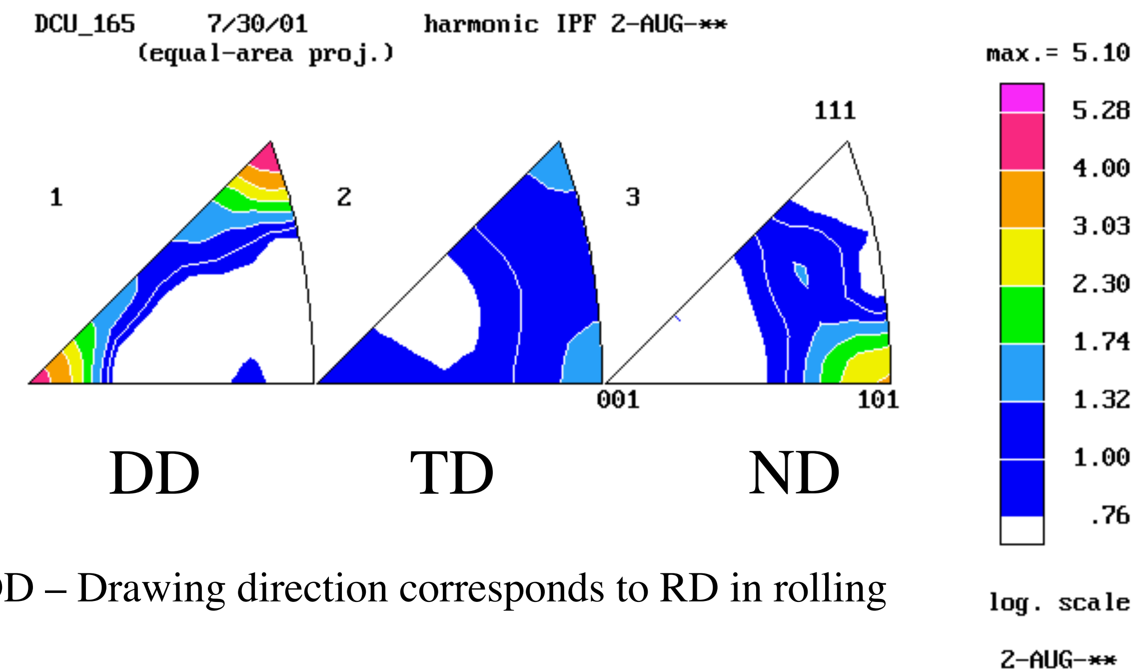

DD – Drawing direction corresponds to RD in rolling

Axisymmetric deformation

- The relative proportions of the two components are determined by the stacking fault energy and vary in a complex manner.

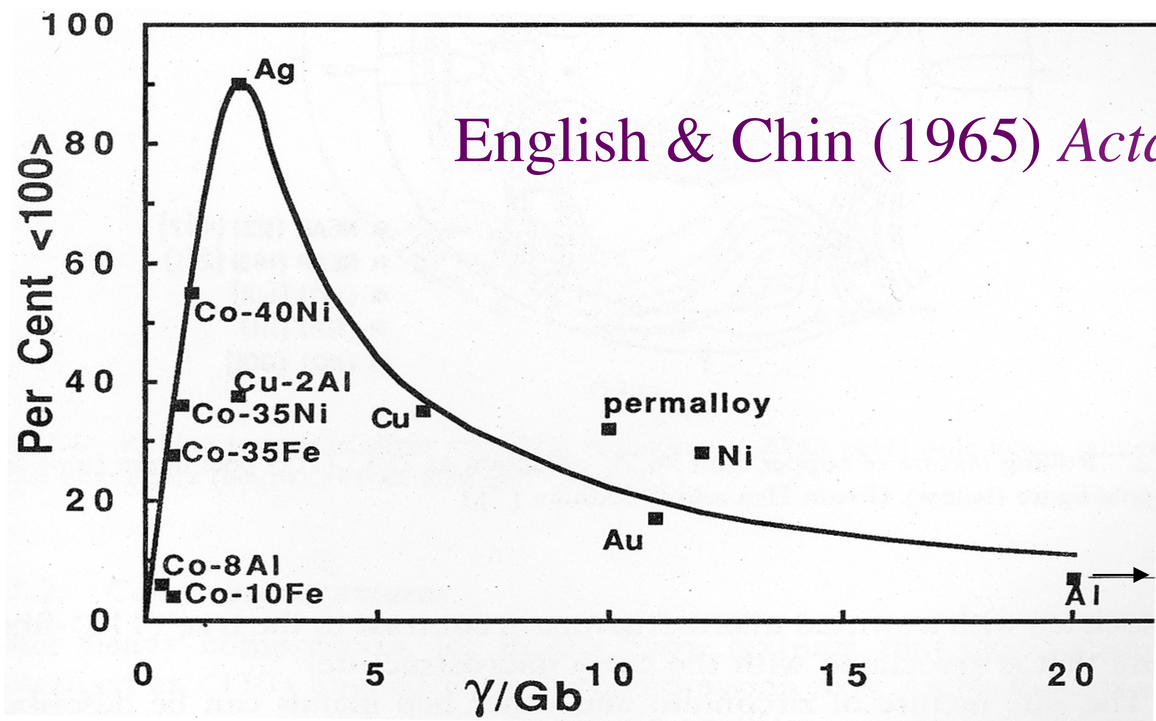

English & Chin (1965) *Acta metall*.

Effect of deformation strain

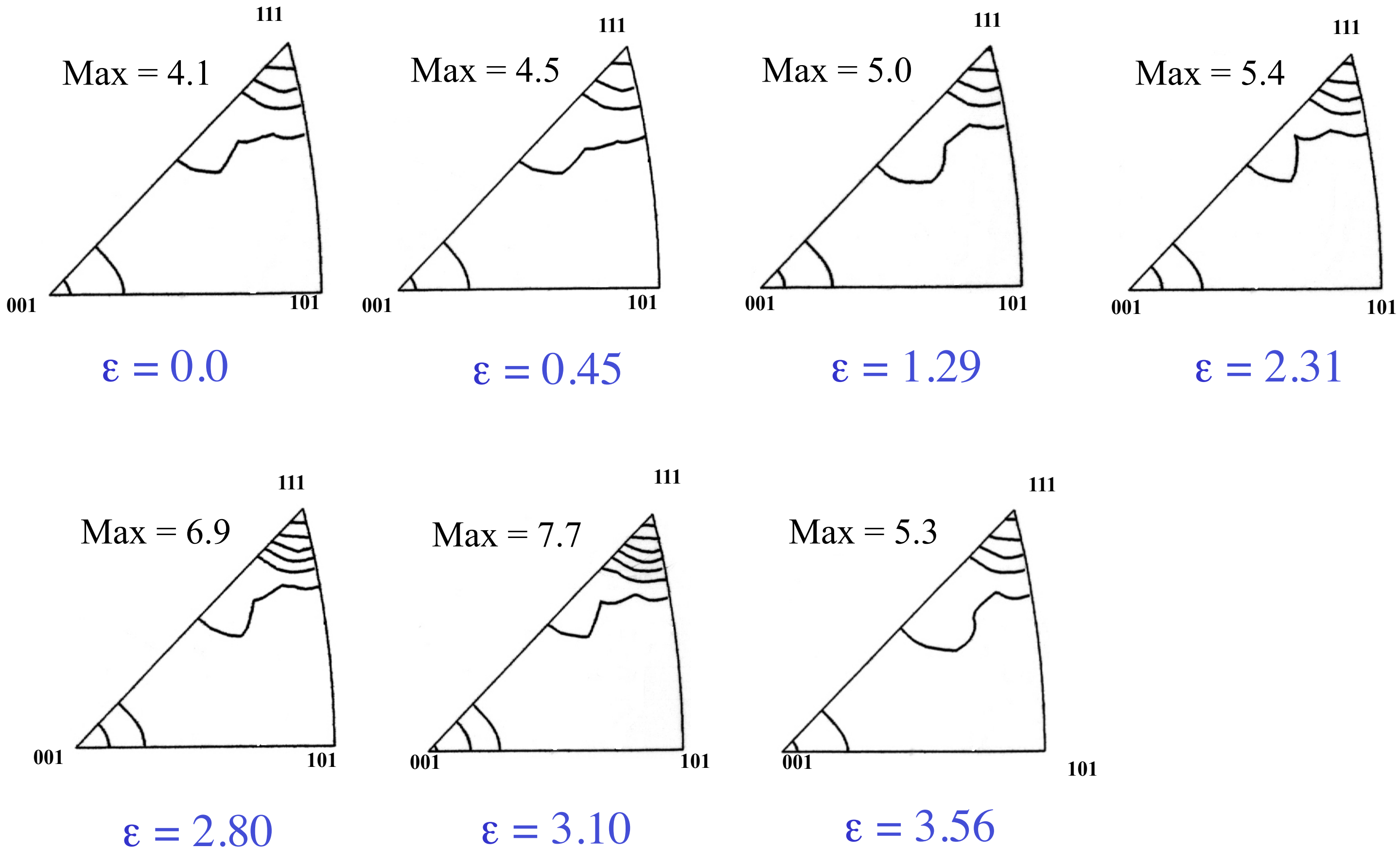

X-ray IPFs showing the effect of strain on the texture of OFHC copper wire

D. R. Waryoba, Ph. D. Dissertation, FSU, 2003

Effect of Temperature

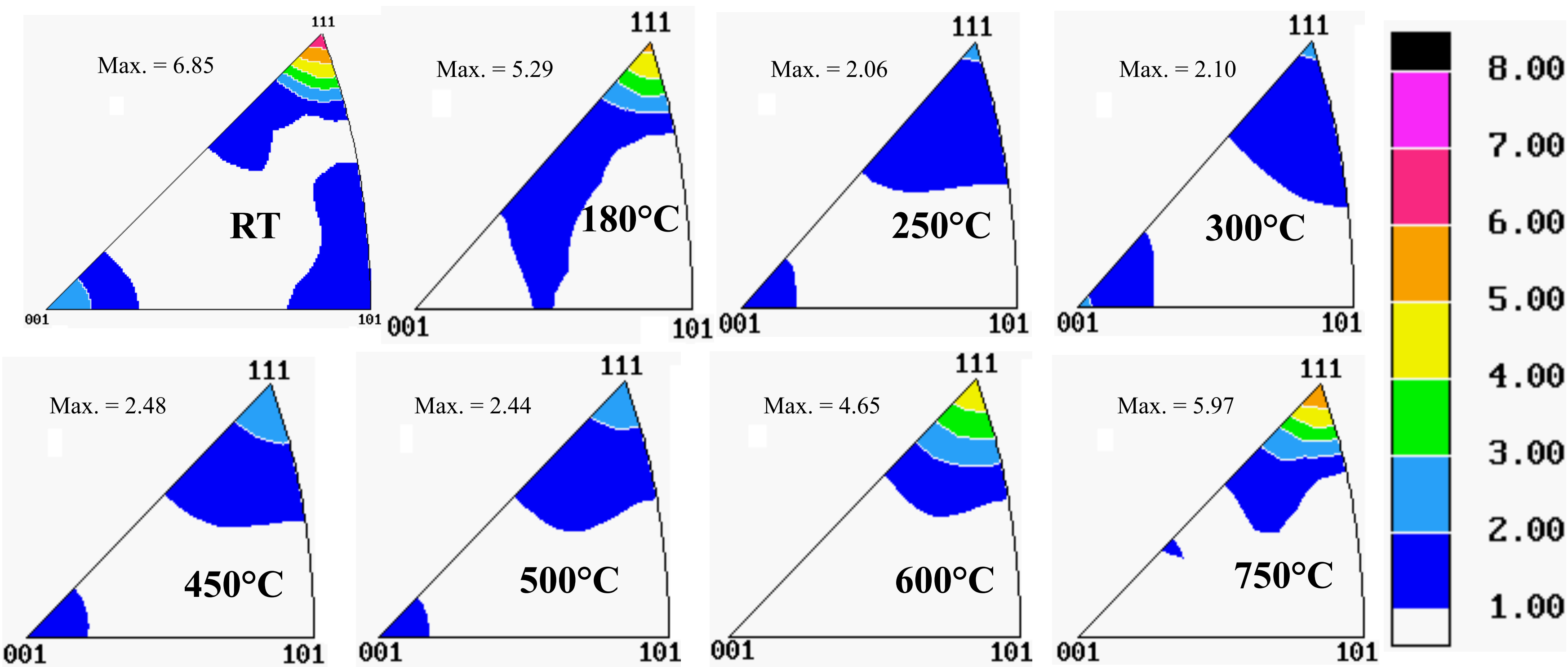

X-ray IPFs showing the effect of annealing temperature on the texture of OFHC copper wire, initially drawn to true strain of 2.31. The strong <111> fiber first decreases with annealing temperature but then increases again.

D. R. Waryoba and P. N. Kalu, TMS 2003,San Diego, CA

Uniaxial Compression: various fcc metals

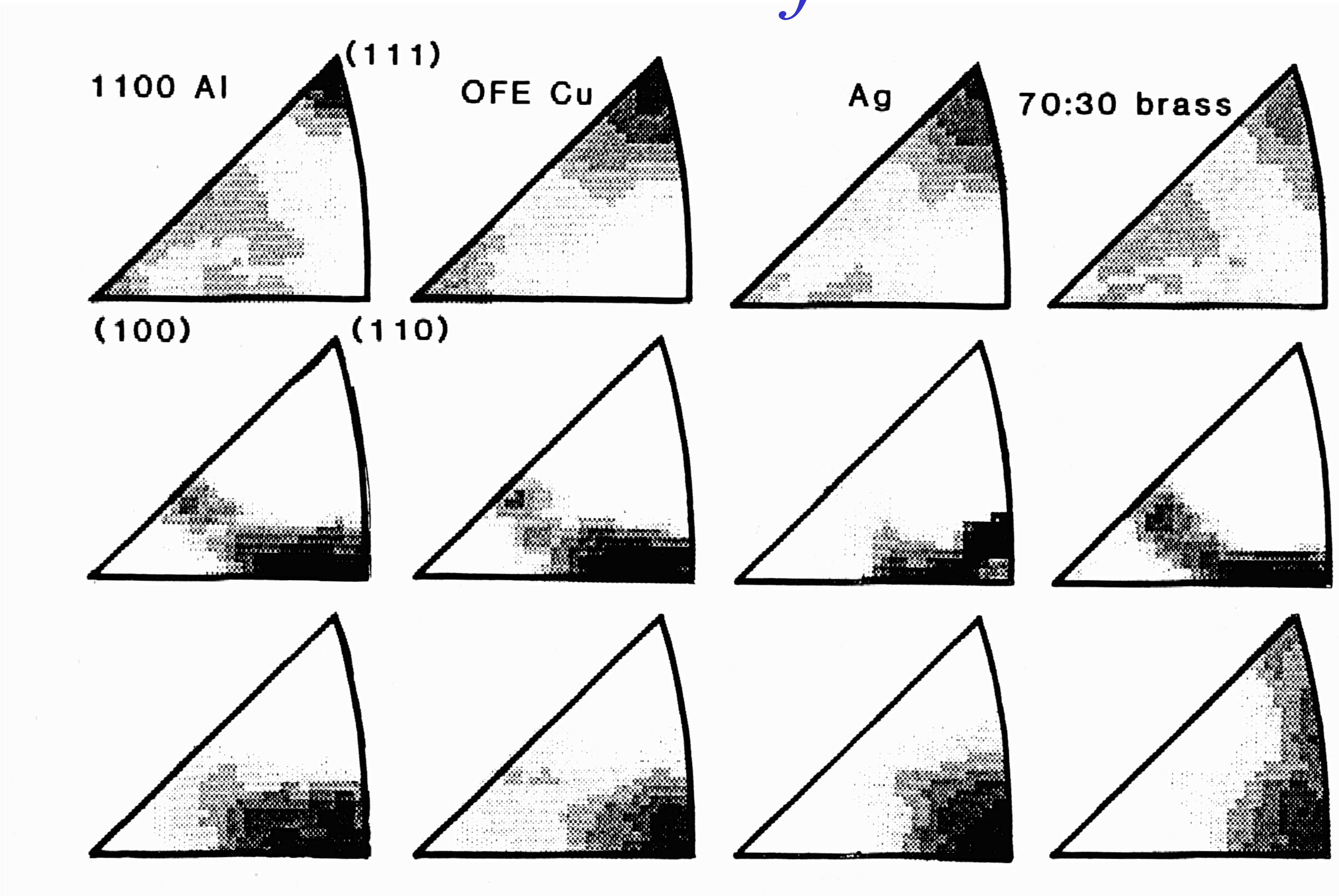

Initial texture

theoretical texture

exptl. texture

[Kocks Ch. 5: Inverse Pole Figures]

BCC uniaxial textures

92% rolled Ta
Tensile test in original RD to strain of 0.6:
<110> fiber

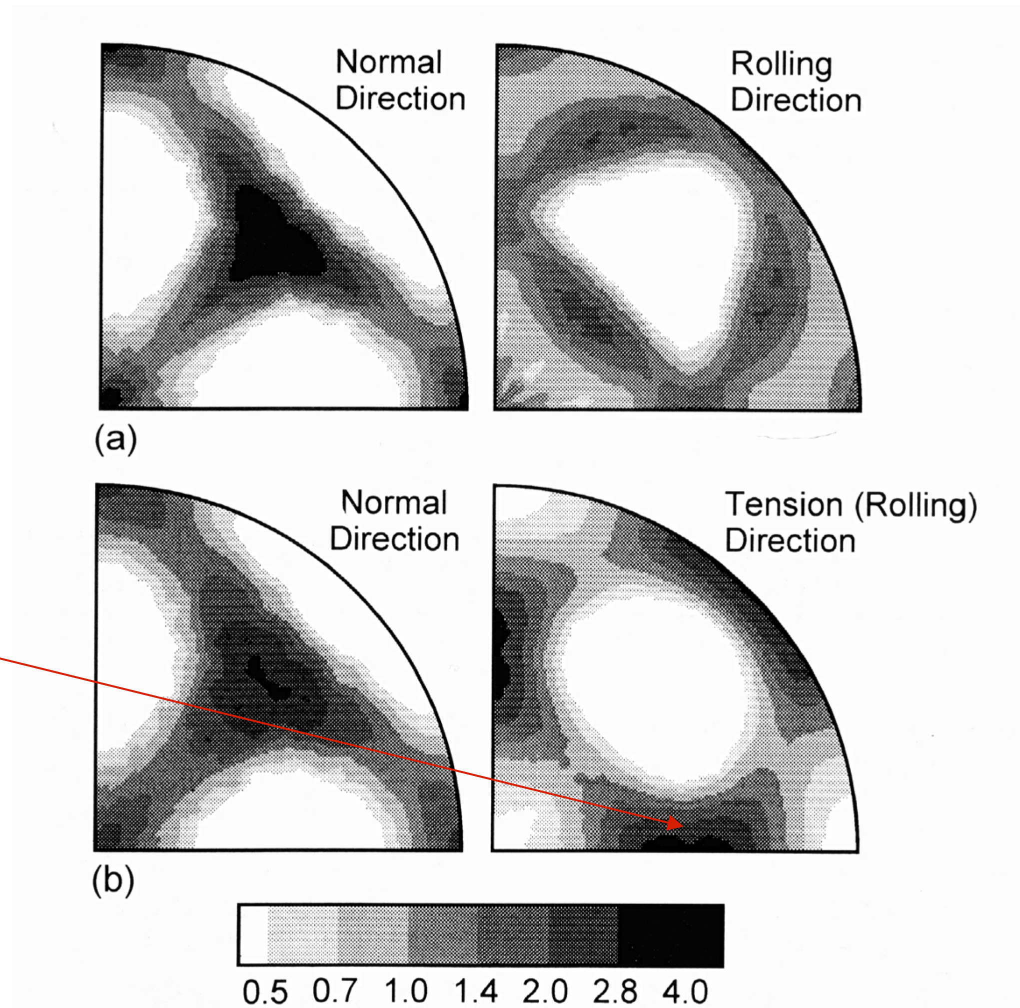

(a) Normal and rolling direction inverse pole figures (equal area projection) of 92% rolled Ta and (b) Prior normal and rolling direction inverse pole figures for (a) tested in tension to a strain of 0.6 (tensile direction coincident to prior rolling direction).

Kocks, Ch. 5

Texture inhomogeneity in Drawn Wires

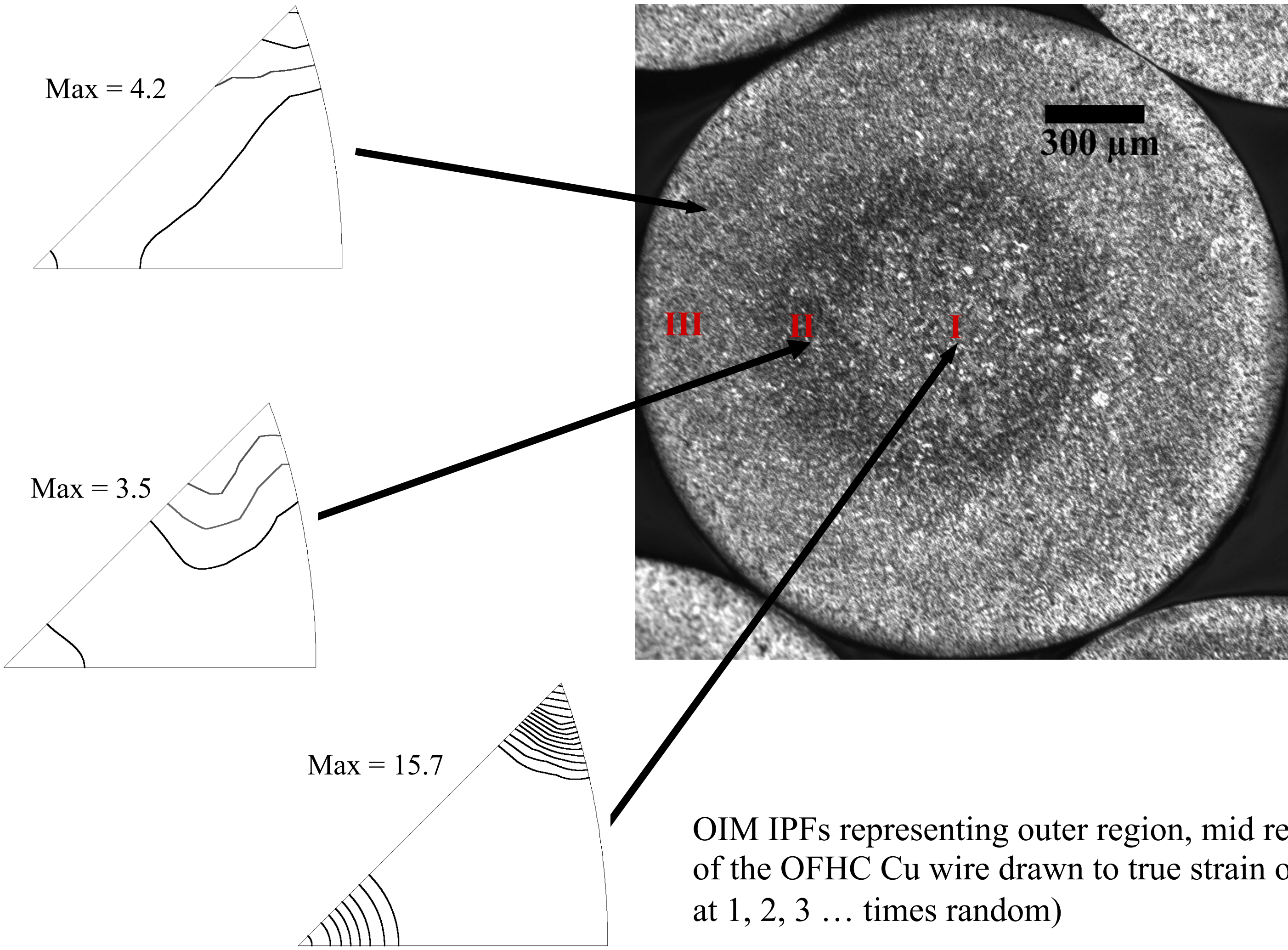

OIM IPFs representing outer region, mid region, and inner core of the OFHC Cu wire drawn to true strain of 2.31 (contours are at 1, 2, 3 … times random)

Texture inhomogeneity in Drawn Wires

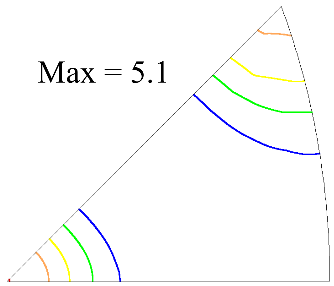

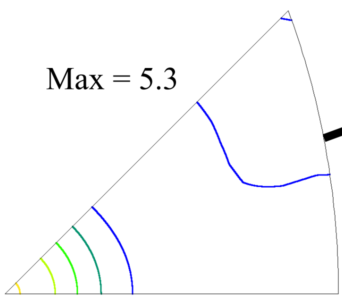

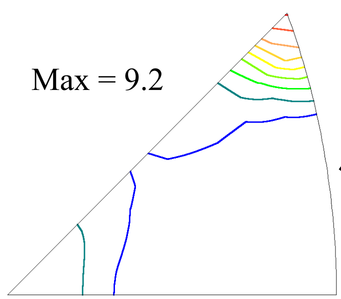

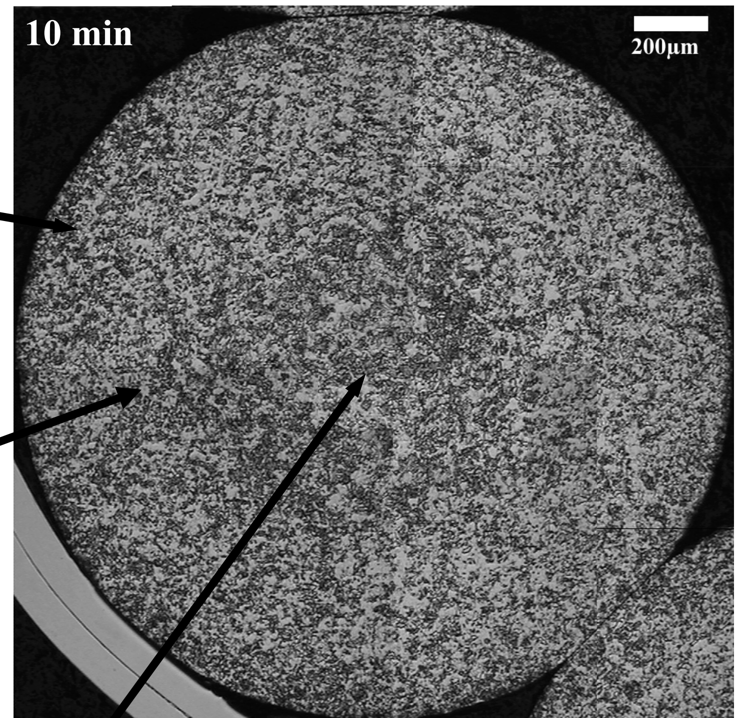

OIM IPFs representing outer region, mid region, and inner core of the OFHC Cu wire drawn to true strain of 2.31 and annealed at 250°C for 10 min (contours are at 1, 2, 3 … times random)

Rolling = Plane Strain

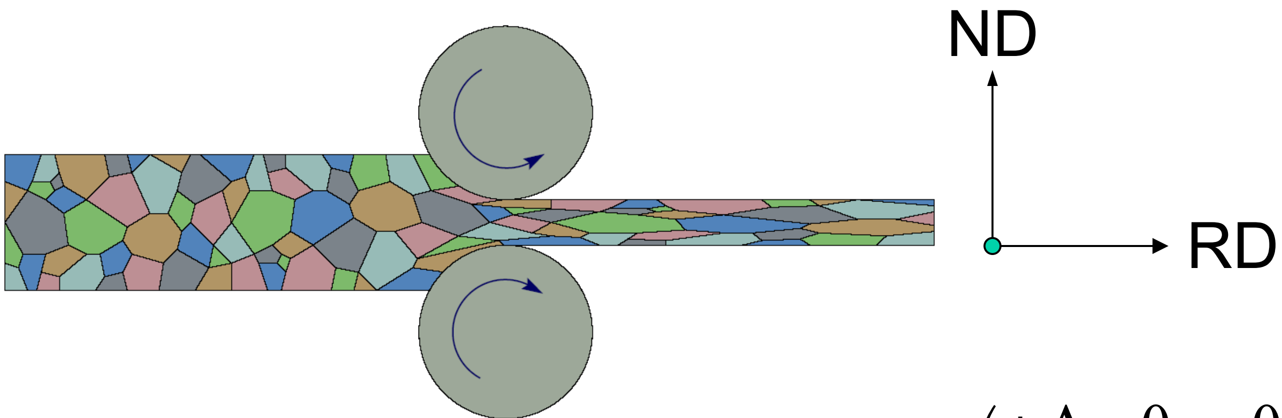

$$\varepsilon = \begin{pmatrix} +\Delta & 0 & 0 \\ 0 & 0 & 0 \\ 0 & 0 & -\Delta \end{pmatrix}$$

Rolling ~ plane strain deformation means extension or compression in a pair of directions with zero strain in the third direction: a *multiaxial strain*.

Plane strain (rolling)

Plane strain means extension/compression in a pair of directions with zero strain in the third direction: a *multiaxial strain*.

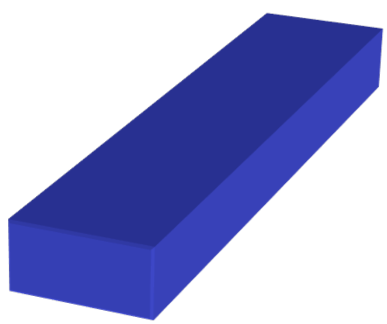

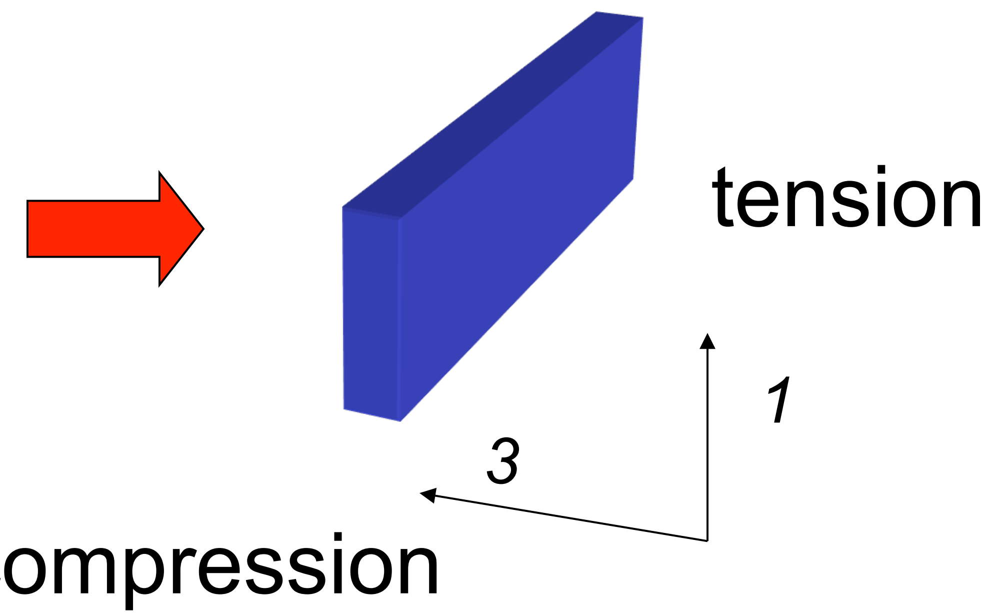

$$d\varepsilon = \begin{pmatrix} +\Delta & 0 & 0 \\ 0 & 0 & 0 \\ 0 & 0 & -\Delta \end{pmatrix}$$

Typical rolling texture in FCC Materials

Type	Component	{hkl}<uvw>	Euler Angles (Bunge)		
			φ_1	θ	φ_2
Deformation	Bs	{011}<211>	35	45	0
	S	{123}<634>	55	35	65
	Cu	{112}<111>	90	30	45
	$Shear_1$	{001}<110>	0	0	45
	$Shear_2$	{111}<110>	0	55	45
	$Shear_3$	{112}<110>	0	35	45
Recrystallization	Goss	{011}<001>	0	45	0
	Cube	{001}<100>	0	0	0
	RC_{RD1}	{013}<100>	0	20	0
	RC_{RD2}	{023}<100>	0	35	0
	RC_{ND1}	{001}<310>	20	0	0
	RC_{ND2}	{001}<320>	35	0	0
	P	{011}<122>	70	45	0
	Q	{013}<231>	55	20	0
	R	{124}<211>	55	75	25

fcc/	bcc/	hcp (Ti)
Shear:		
A:{111}<uvw>	E:{110}<001>	?
B:{hkl}<110>	D:{112}<110>	
C: {001}<110>		
Rolling: Partial Fibers:		
beta, alpha	gamma, alpha	{0001} split to +/-TD

Fcc rolling textures

- The next set of slides summarizes rolling textures in fcc metals. This topic was also presented as an example in the discussion of Orientation Distributions and their graphical representation.

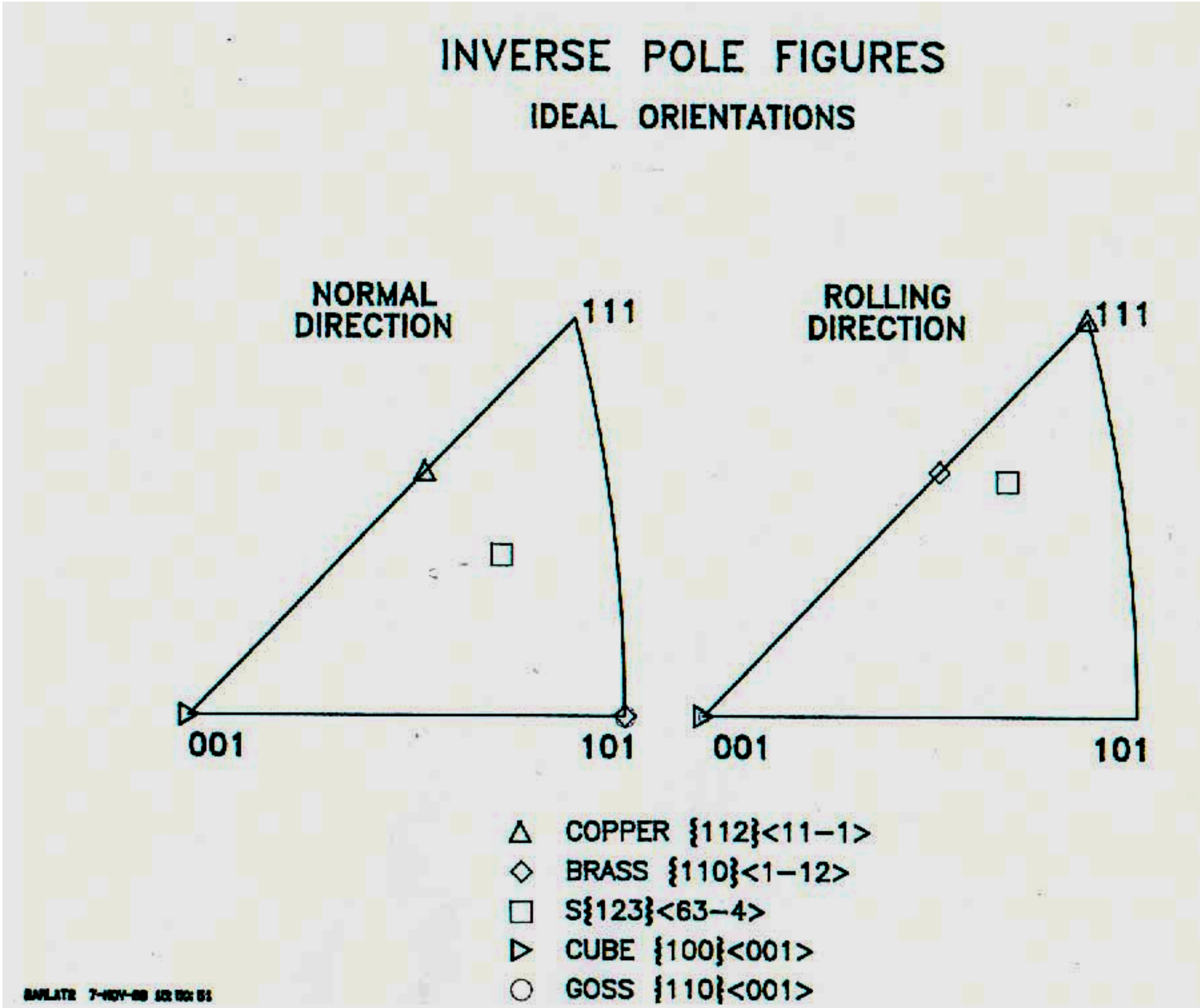

INVERSE POLE FIGURES
IDEAL ORIENTATIONS
NORMAL DIRECTION
ROLLING DIRECTION
111
001
101
111
001
101
COPPER {112}<11-1>
BRASS {110}<1-12>
S{123}<63-4>
CUBE {100}<001>
GOSS {110}<001>

Cartesian Euler Space

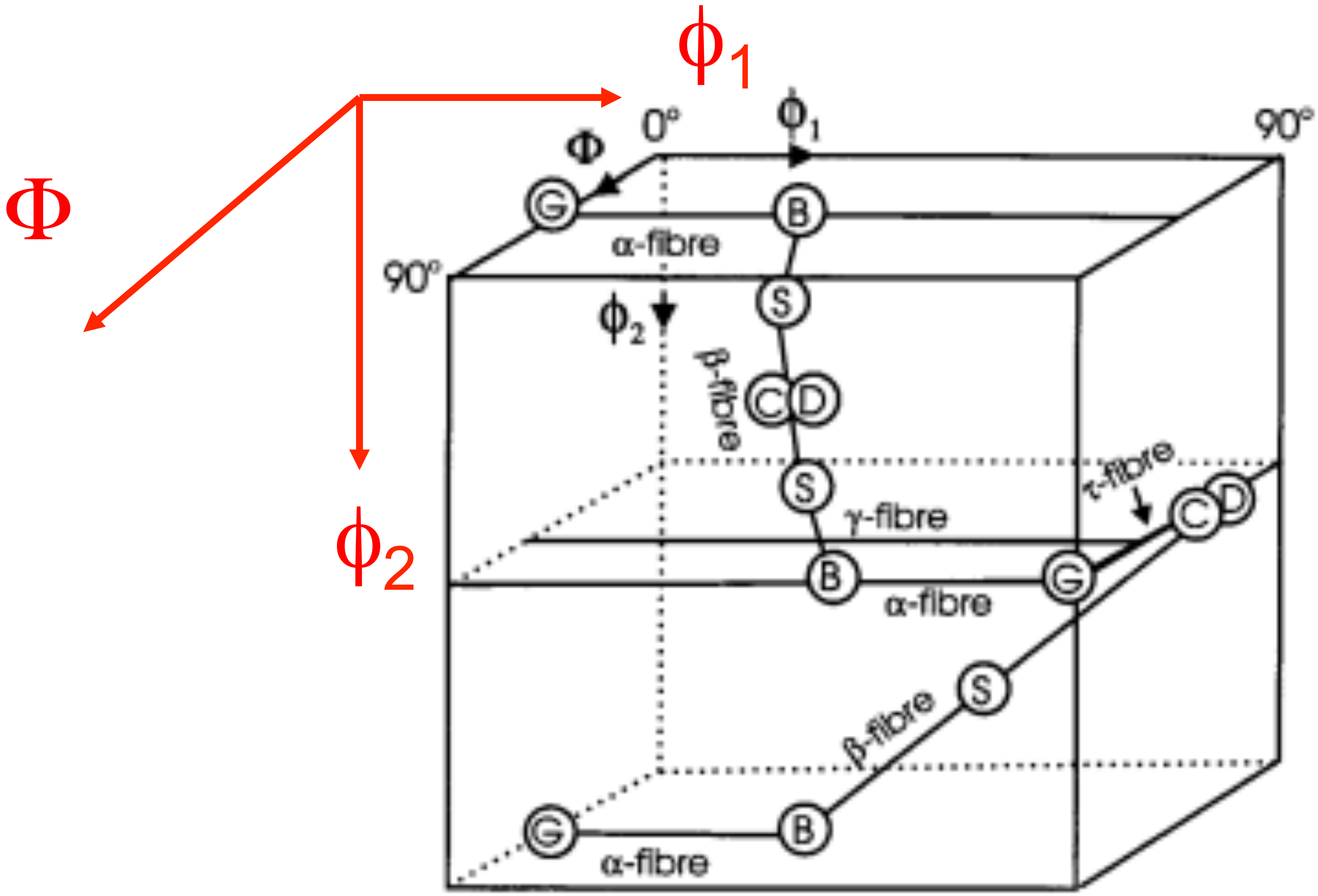

Sections

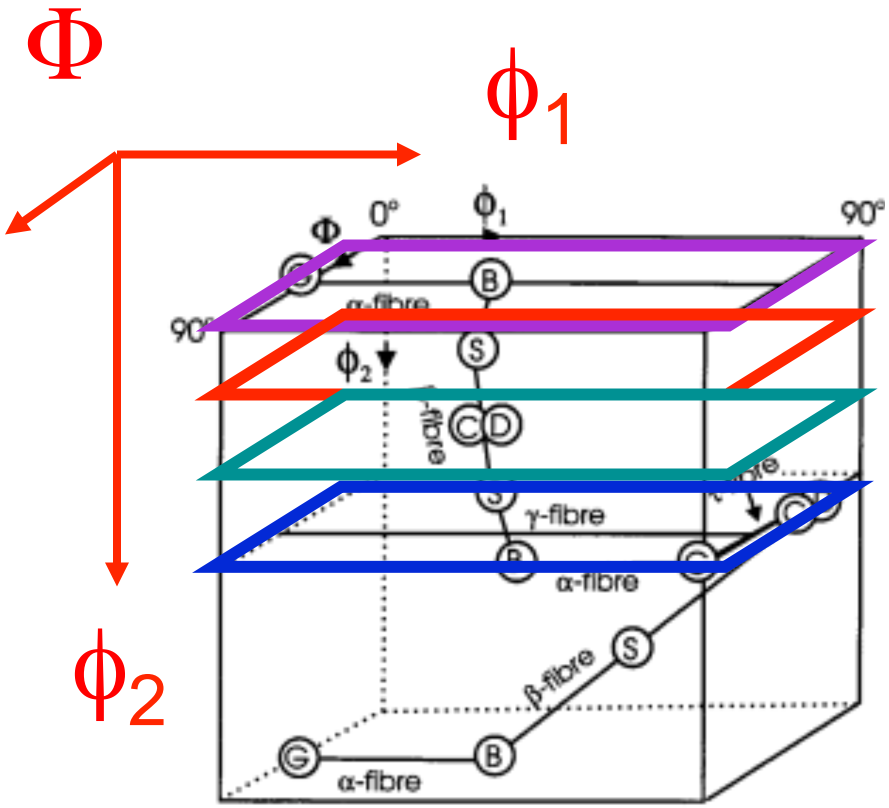

Φ
φ1
φ2
0°
90°
α-fibre
γ-fibre
β-fibre

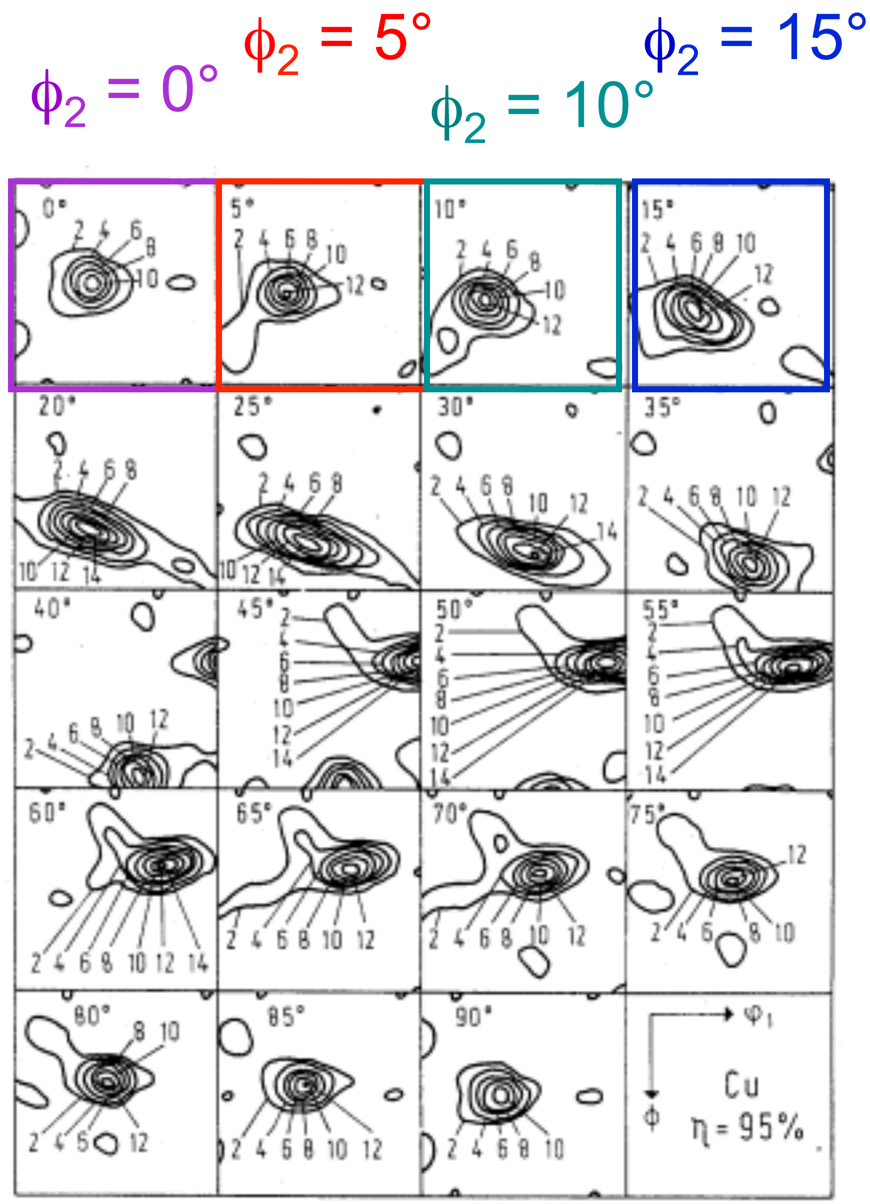

φ2 = 0°
φ2 = 5°
φ2 = 10°
φ2 = 15°
0°
5°
10°
15°
20°
25°
30°
35°
40°
45°
50°
55°
60°
65°
70°
75°
80°
85°
90°
φ1
Φ
Cu
η = 95%

PF Representation

Name	Indices	Bunge (φ_1,Φ,φ_2)
▲ copper	{112}<11$\bar{1}$>	90°, 35°, 45°
● S1	{124}<21$\bar{1}$>	59°, 29°, 63°
● S2	{123}<41$\bar{2}$>	47°, 37°, 63°
● S3*	{123}<63$\bar{4}$>	59°, 37°, 63°
◆ brass	{110}<$\bar{1}$12>	35°, 45°, 0°
Taylor	{4 4 11}<11 11 $\bar{8}$>	7°, 71°, 70°
■ Goss	{110}<001>	0°, 45°, 0°

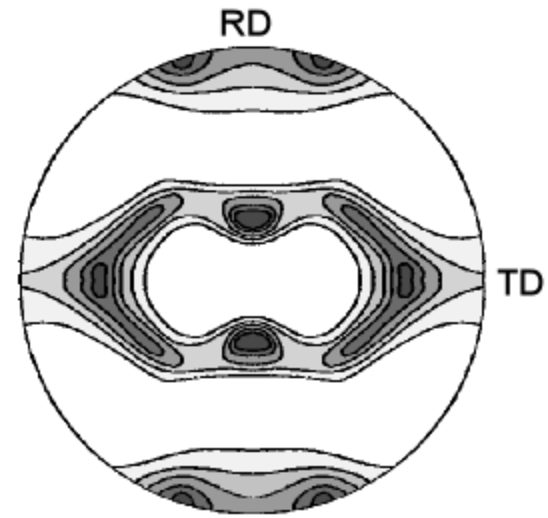

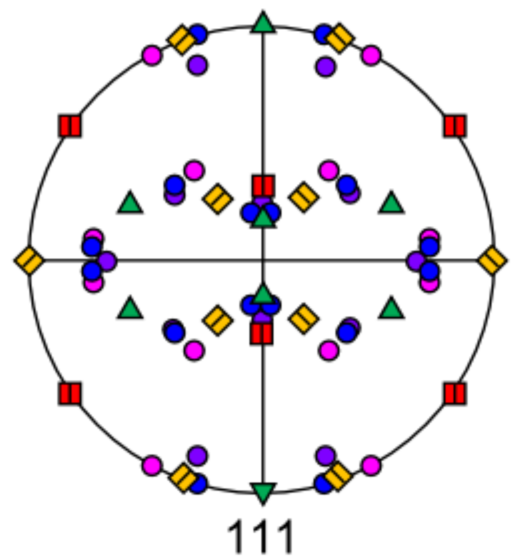

Note how very different components tend to overlap in a pole figure.

Fiber Plots:

various rolling reductions:
(a) intensity versus position along the fiber
(b) angular position of intensity maximum versus position along the fiber

Kocks, Ch. 2

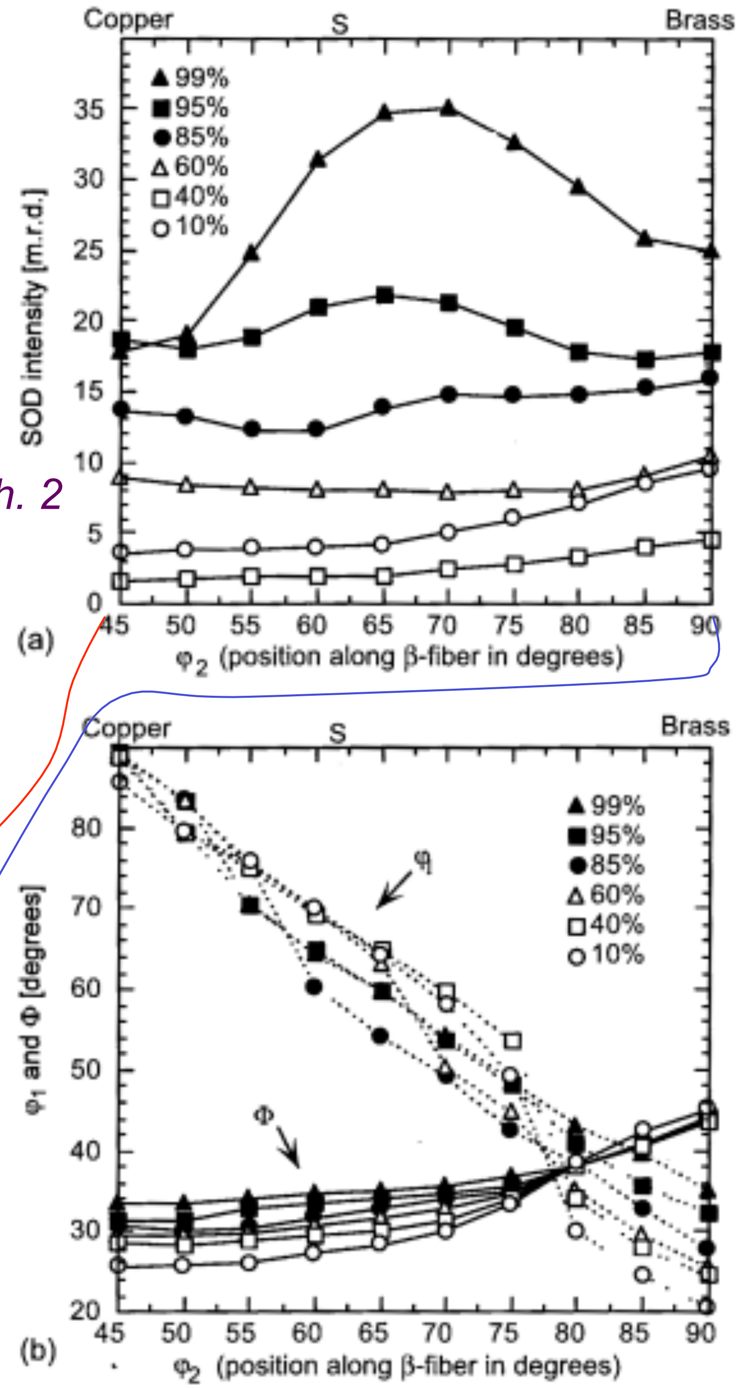

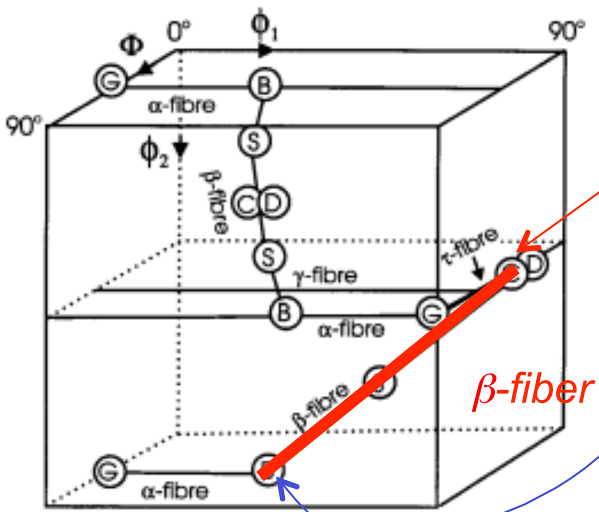

Volume fraction vs. density (intensity)

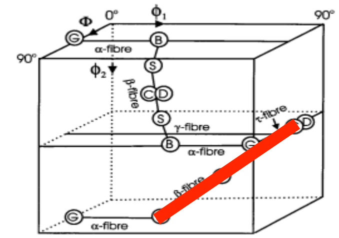

- Volume fraction associated with region around the fiber in a given section.
- V_f increases faster than density with increasing Φ.
- Location of max. density not at nominal location.

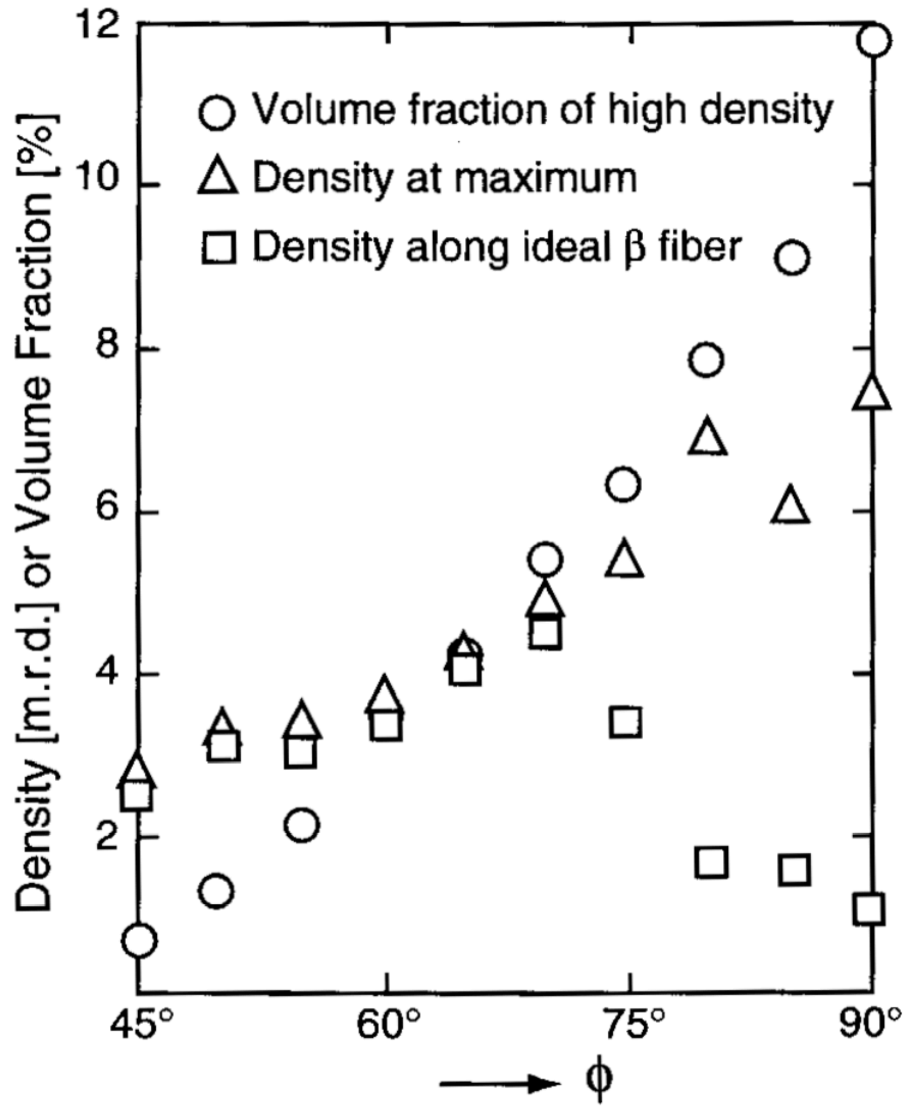

Kocks, Tomé, Wenk: Ch. 2

Rolling fcc Cu: Effect of Strain

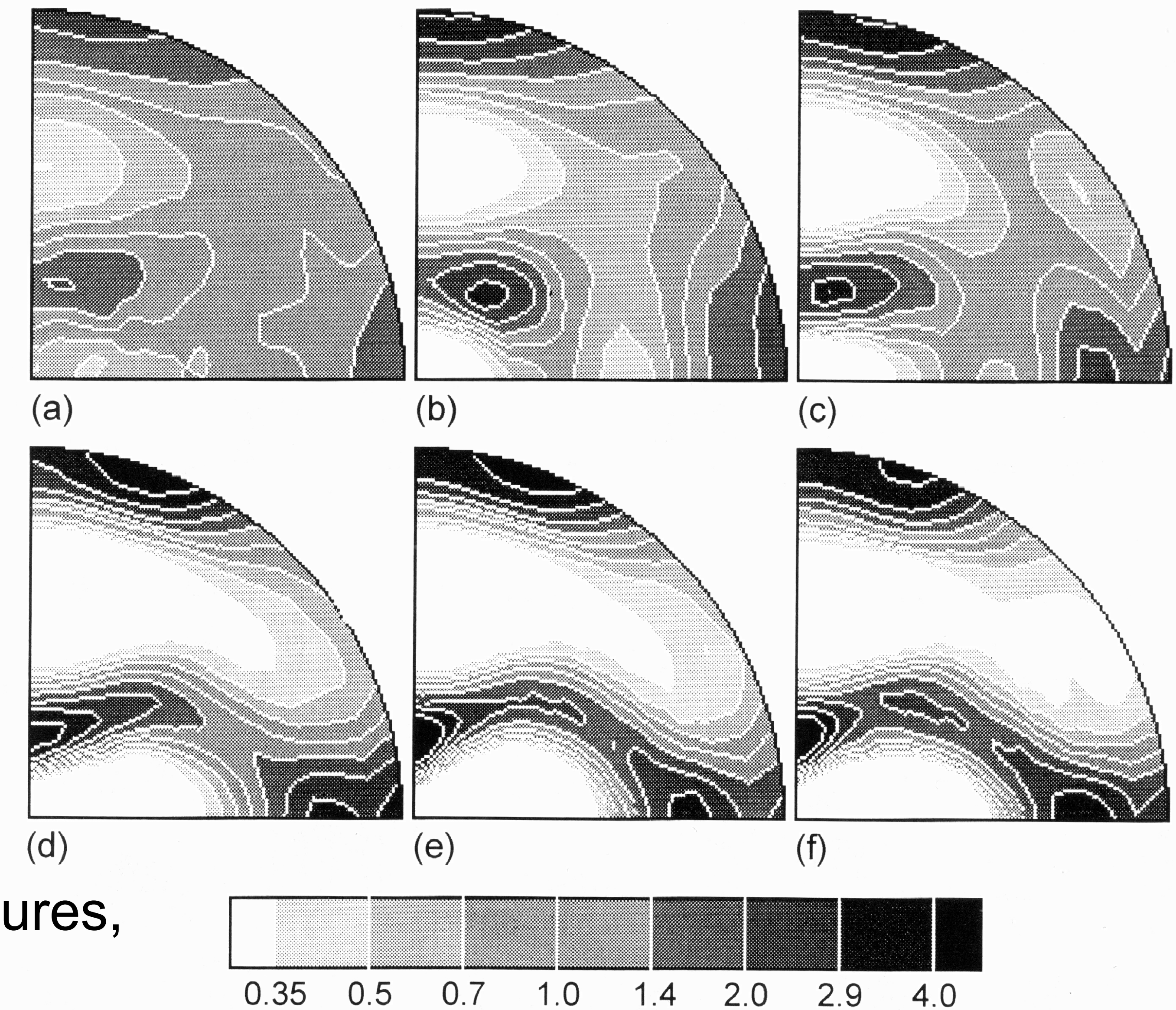

{111} Pole Figures, RD vertical

von Mises strains= initial, 0.5, 1.0, 2.0, 2.7, 3.5

Effect of Alloying: Cu-Zn (brass); the texture transition

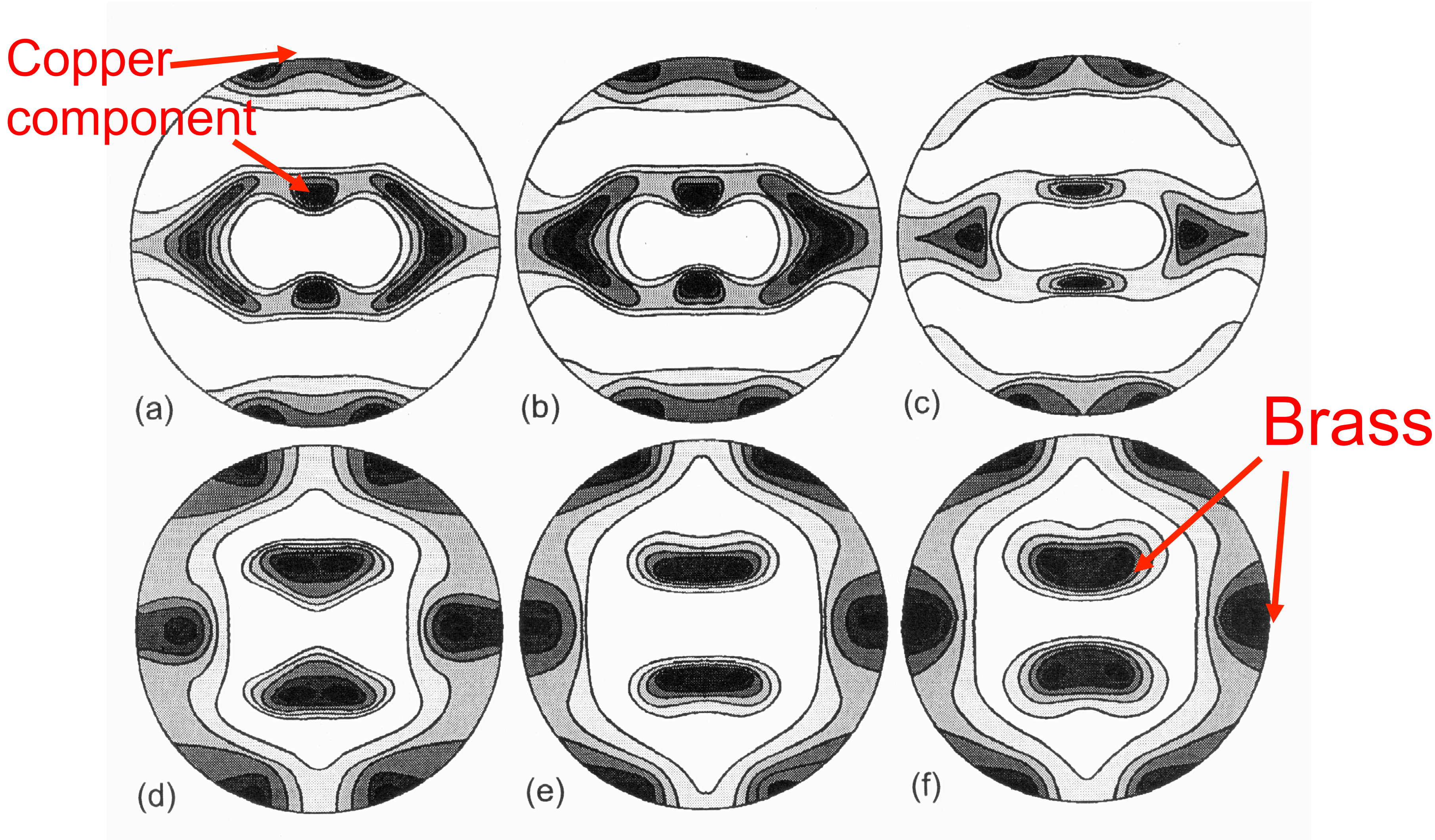

Zn content: (a) 0%, (b) 2.5%, (c) 5%, (d) 10%, (e) 20% and (f) 30% [Stephens PhD, U Arizona, 1968]

Alloy, Precipitation Effects

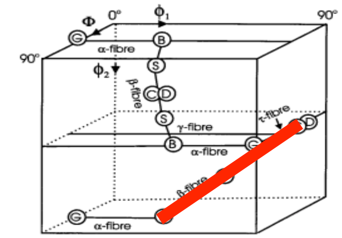

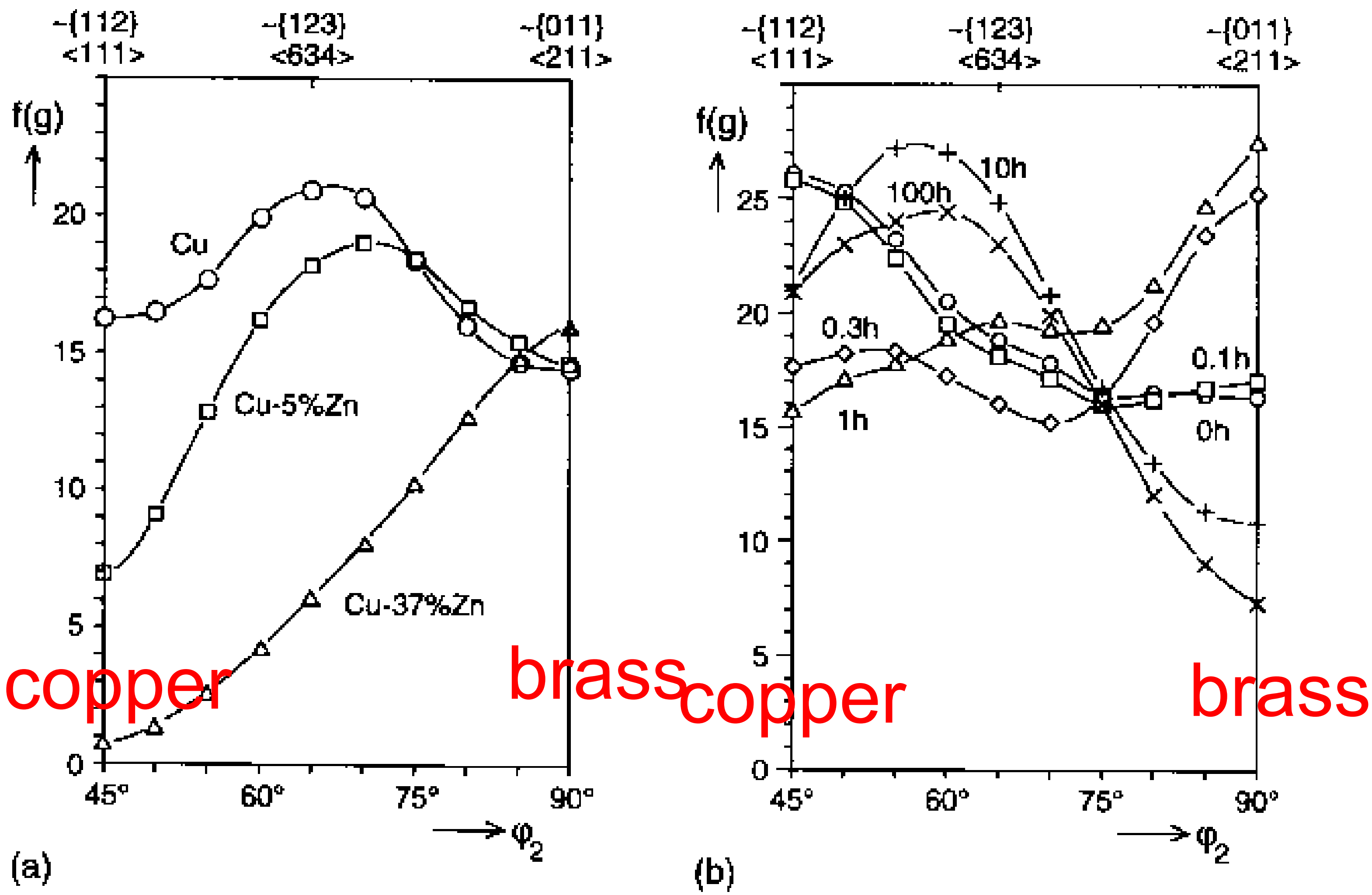

Hirsch & Lücke, 1988 , Acta metall. **36**, 2863

Engler et al., 1989, Acta metall. **37**, 2743

Rolling Textures BCC

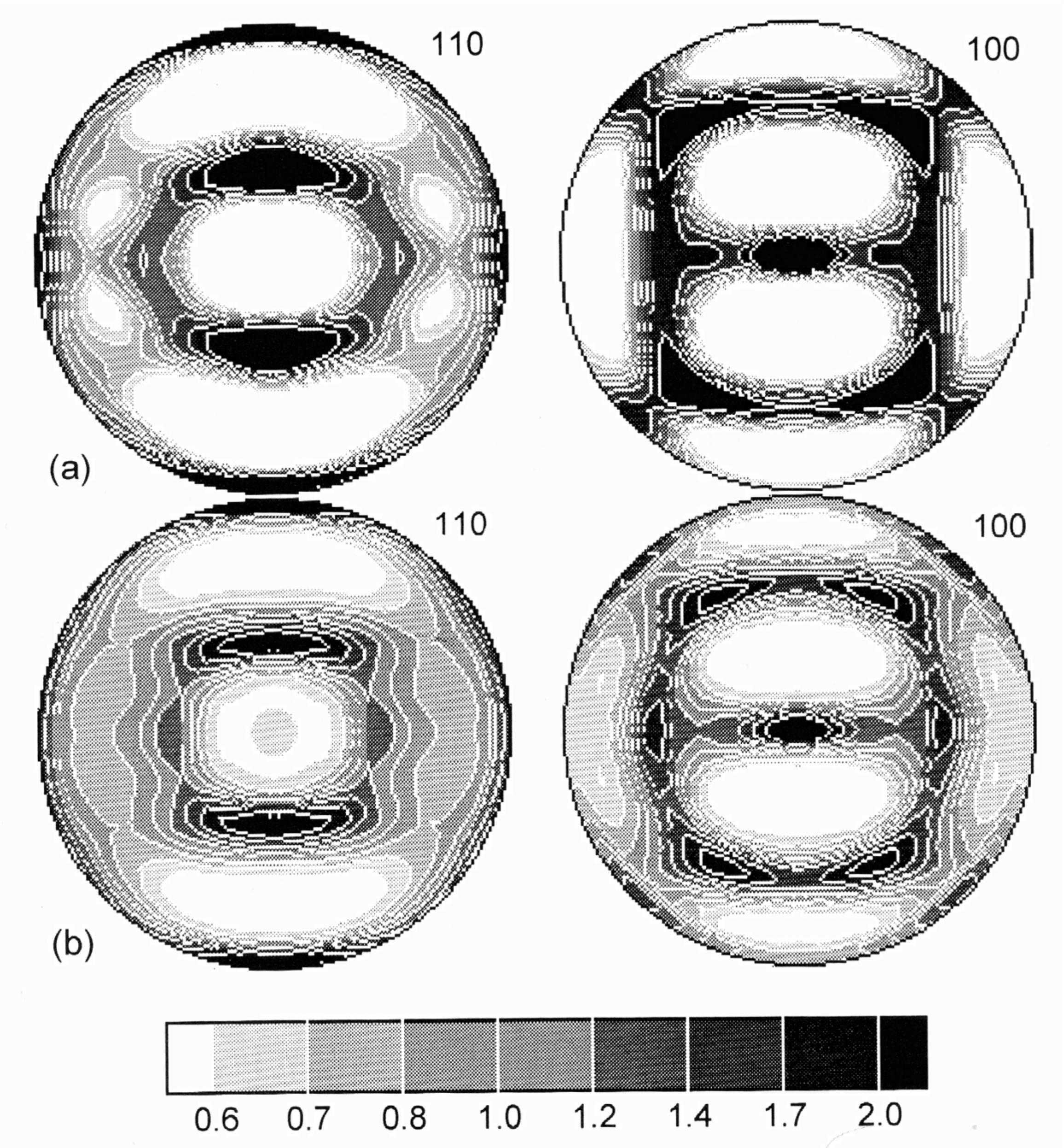

{110} and {100} pole figures (equal area projection; rolling direction vertical) for (a) low-carbon steel cold rolled to a reduction in thickness of 80% (approximate equivalent strain of 2); (b) tantalum, unidirectionally rolled at room temperature to a reduction in thickness of 91%.

Kocks, Ch. 5

{100} Pole figure for certain components of rolled BCC metals

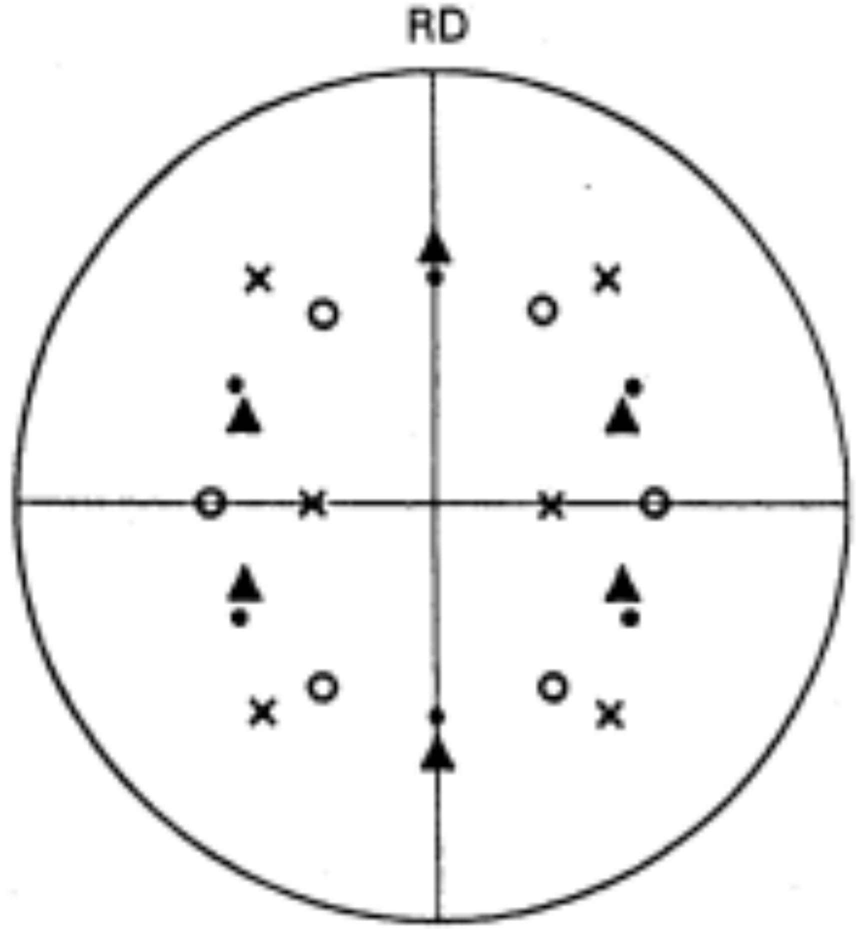

Note how very different components tend to overlap in a pole figure.

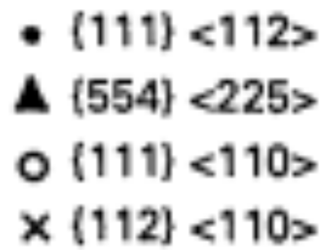

Kocks, Ch. 5

BCC fibers: the $\phi_2 = 45°$ section

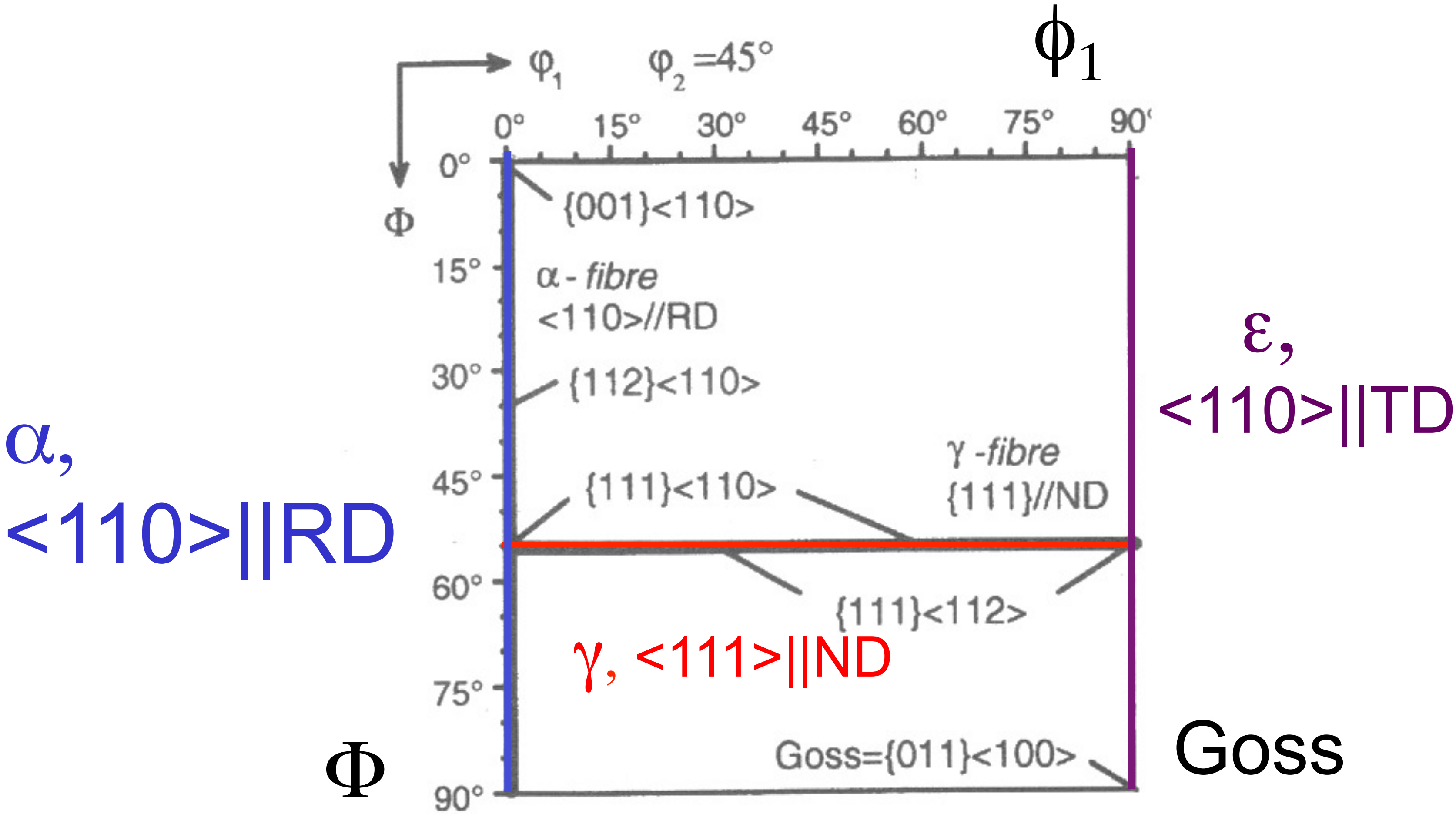

Ta, Fe rolling textures

Note: Euler angles are Roe angles: axes transposed with Θ horiz., ψ vertical.

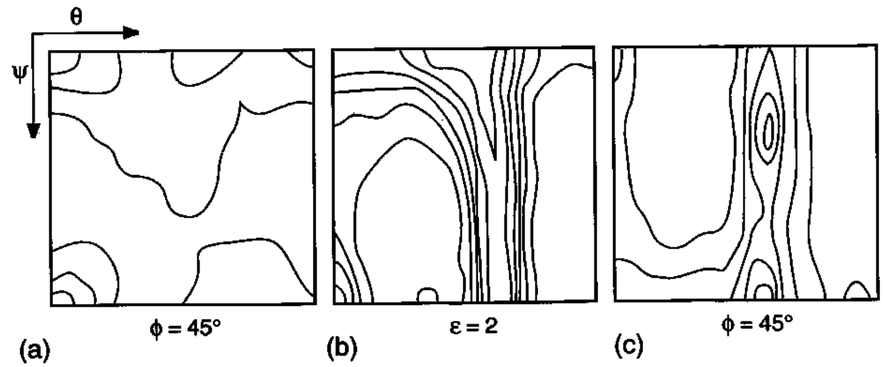

Fig. 15. Plot of the 45° sections (ϕ_2=45°, Roe angles) for the same steel and tantalum textures shown in Fig. 13: (a) low-carbon steel prior to cold rolling; (b) low-carbon steel cold rolled to a reduction in thickness of 80% (approximate equivalent strain of 2); (c) tantalum, unidirectionally rolled at room temperature to a reduction of 91%. The contours are drawn at multiples of the random intensity of 1,2,3...7. Note the weaker intensities in the tantalum, and the stronger α fiber in the steel.

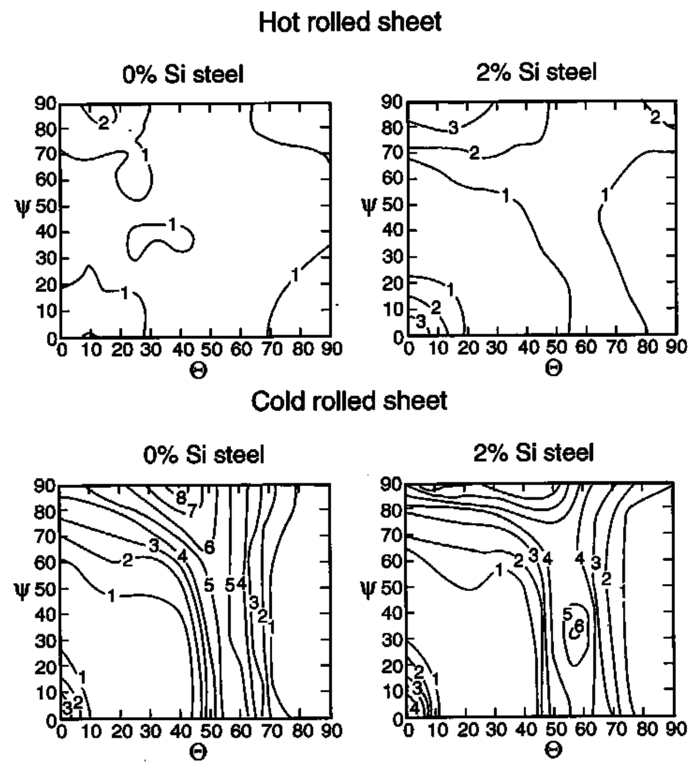

Fig. 16. Plot of the 45° sections (ϕ_2=45°, Roe angles, origin in lower left corner) for steels with 0% and 2% Si, both as hot-rolled (initial condition) and after 75% reduction cold rolling. The strongest intensity is at the {112}⟨110⟩ position in the 0% Si-steel, whereas it is at the {111}⟨110⟩ position in the 2% Si-steel. Note that a weak RD||⟨110⟩ fiber is already present in the hot rolled 2% Si-steel.

Fe, Fe-Si rolling fiber plots

Note the marked alloy dependence in the alpha fiber; smaller variations in the gamma fiber.

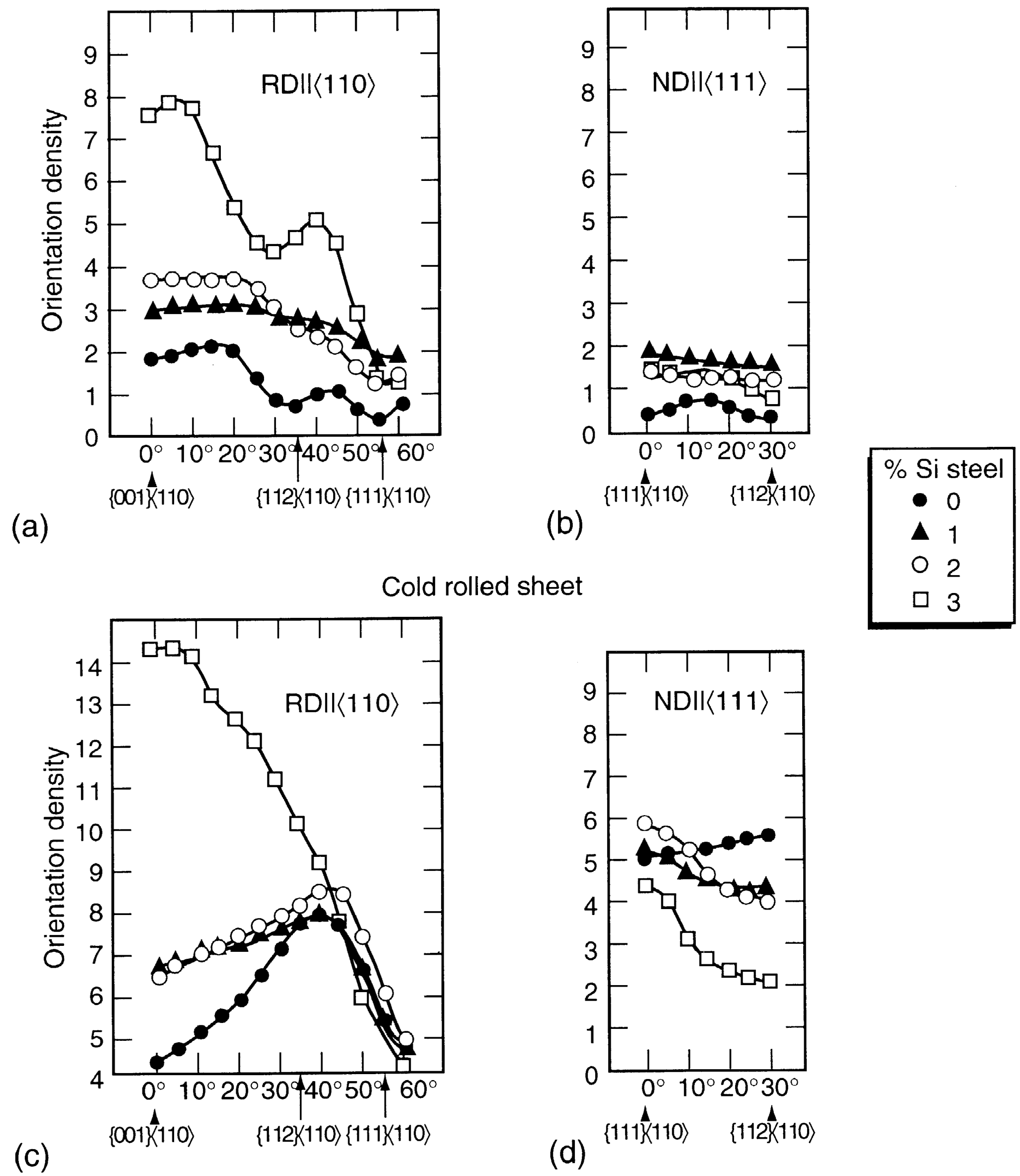

Fig. 17. Plot of the α and γ fibers for a range of iron-Si alloys, including 0, 1, 2, & 3% Si. Increasing silicon leads to stronger α fibers in both the hot-rolled (initial) condition and the cold-rolled condition.

Summary: part 1

- Typical textures illustrated for FCC & BCC metals as a function of alloy type (stacking fault energy) and deformation character (strain type).
- Pole figures are recognizable for standard deformation histories but orientation distributions provide much more detailed information. Inverse pole figures are also useful, especially for uniaxial textures.
- Measure strain using von Mises equivalent strain.
- Plane strain (rolling) textures concentrate on characteristic lines ("partial fibers") in orientation space.
- Uniaxial textures align certain crystal axes with the deformation axis.

Part 2: shear/ torsion textures

- This section covers shear (torsion) textures

Shear Texture

- Shear strain means that displacements are tangential to the direction in which they increase.
- Shear direction=1, Shear Plane ⊥ 2-axis
- The matrix shows the velocity gradient; the strain (rate) is the symmetrized version of *L*.

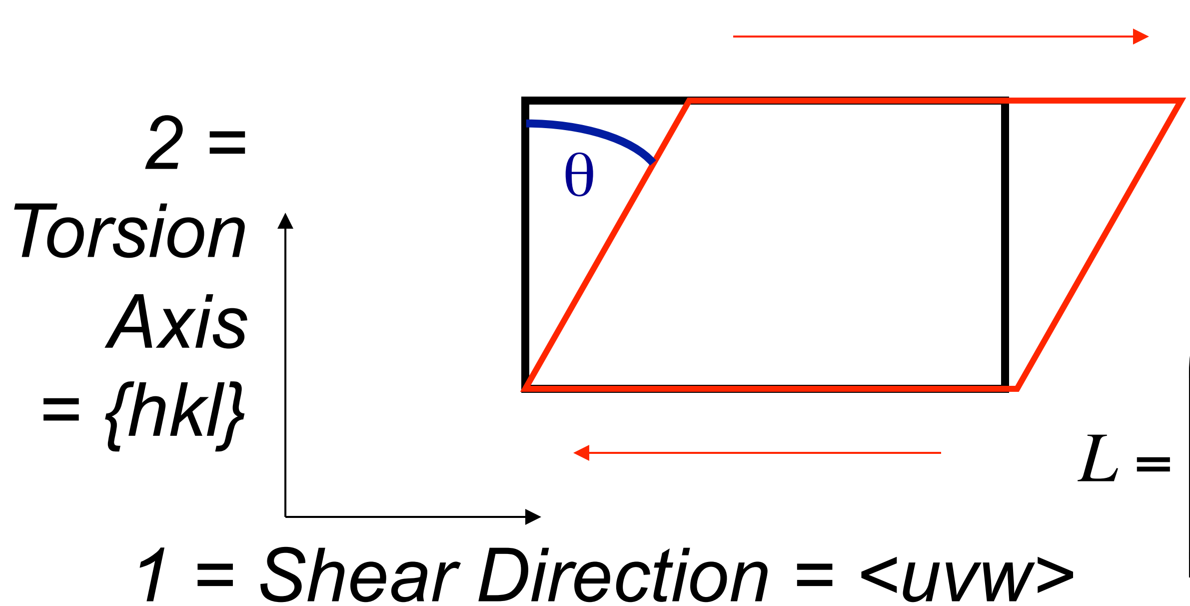

$\varepsilon_{12} = \tan\theta$

Note the definition of strain, ε_{ij}, as the derivative of the displacement u_i with respect to coordinate x_j.

$$L = \begin{pmatrix} 0 & +\Delta & 0 \\ 0 & 0 & 0 \\ 0 & 0 & 0 \end{pmatrix}$$

Torsion Textures: twisting of a hollow cylinder specimen

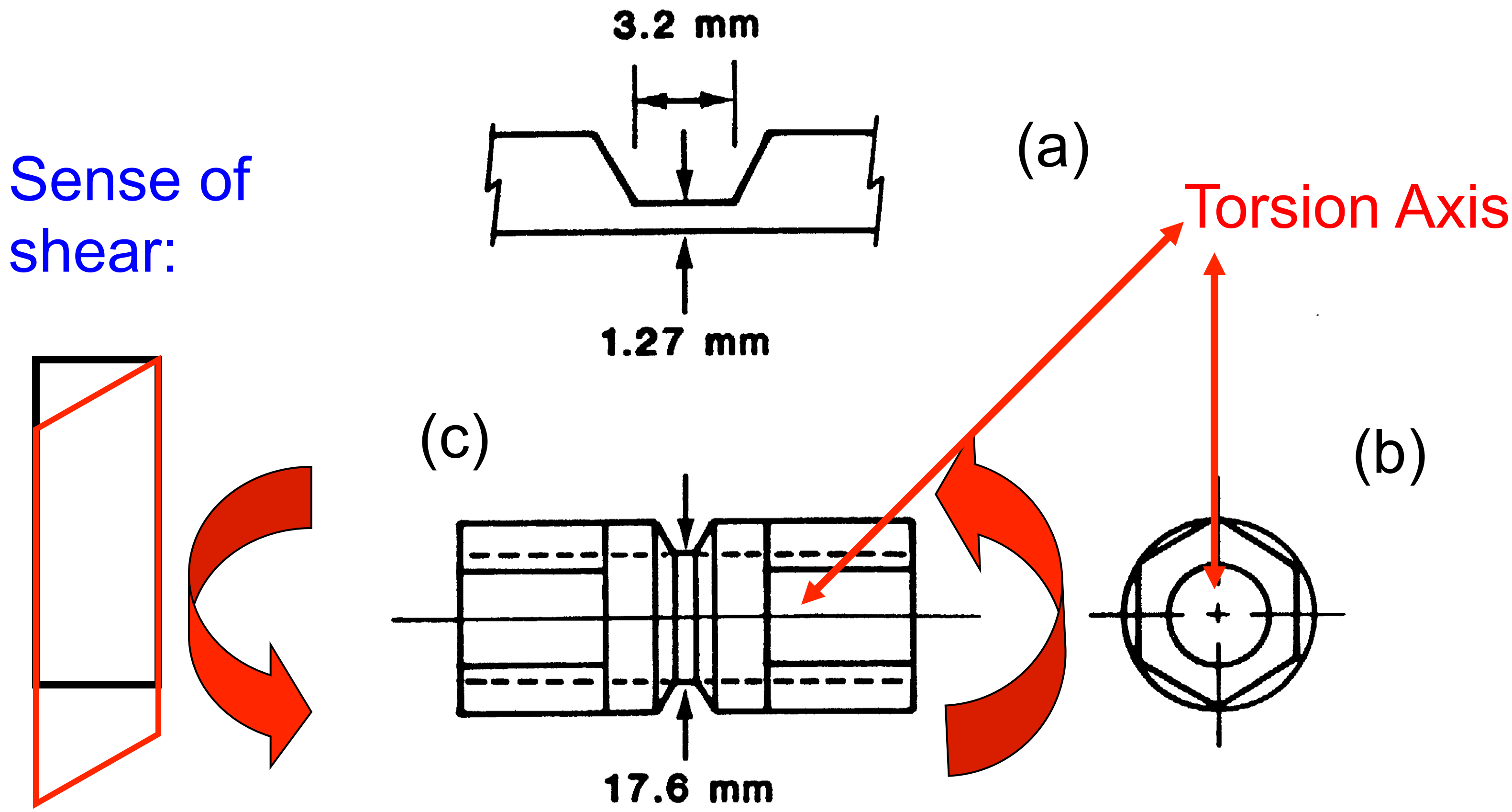

Torsion Axis

Shear Textures: idealized texture components for FCC *metals*

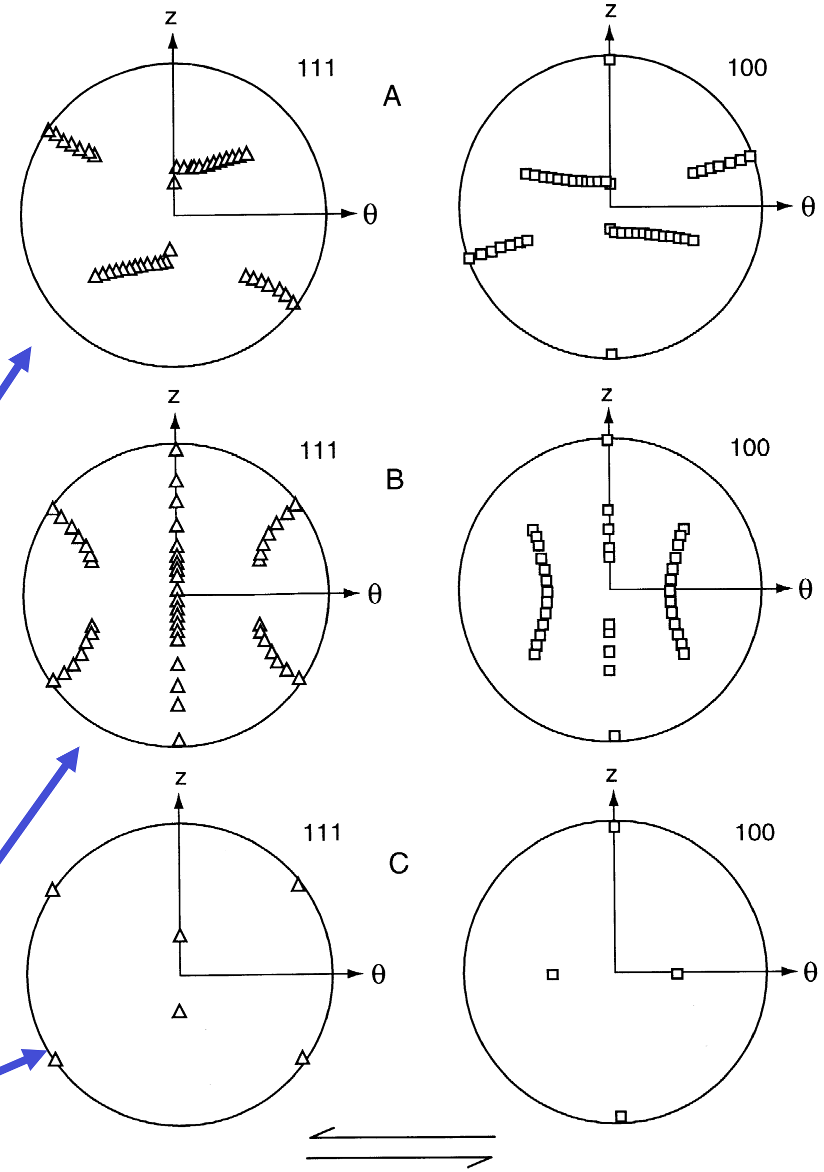

A partial fiber {111}<uvw>

B partial fiber {hkl}<110>

C component: {001}<110>

Canova *et al*. (1982), 'Texture Development Prediction for Deformation in Torsion and Tension at Large Strains', *J. Metals* **35** A21-A21; Canova *et al*. (1984), 'Theory of Torsion Texture Development', *Acta metall*. **32** 211

Shear direction

FCC Torsion Textures

Plots of {111} and {200} pole figures (equal area projection; torsion axis vertical) for the following materials deformed in torsion; the shear direction points to the left in these figures.

a) Nickel at γ=3.6
b) Copper at γ=3.5
c) Silver at γ=3.5
d) Cu-30Zn at γ=3.5
e) Ni-60Co at γ=3.2

Note that the partial "A" fiber is present in Ni and Cu, but is absent in the other materials. Silver, brass and Ni-60Co show instead a "D" fiber which is similar to the A fiber but rotated approximately 90° about the torsion axis. The B fiber is present to varying degrees in all the materials.

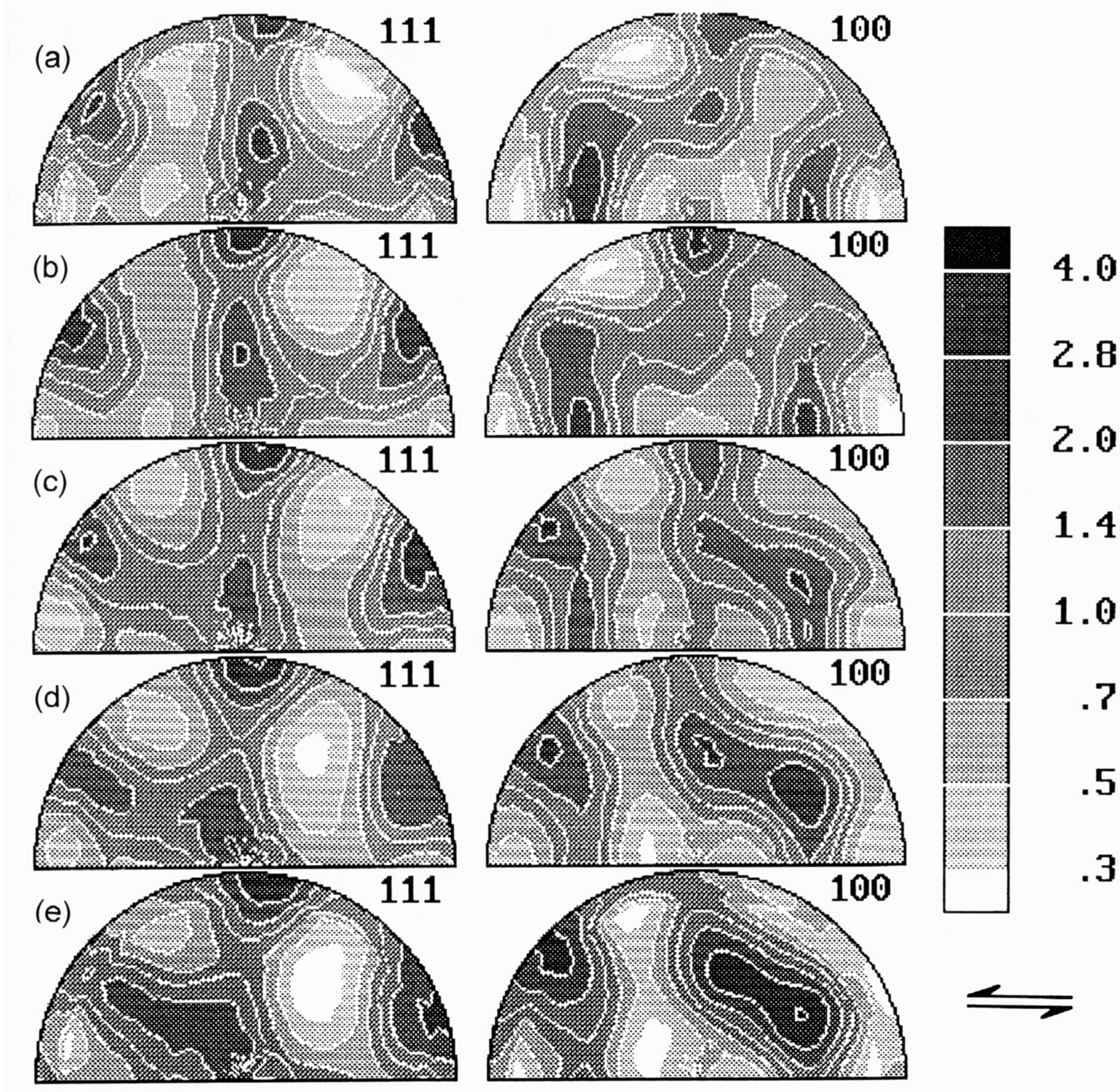

Kocks, Ch. 5

Shear Texture Components

- Why study shear textures? Shear strain is common near the surface of rolled parts, for example.
- Partial Fibers: A/D {111}<uvw>…<110>

Partial Fibers:	A/D	{111}<uvw>…<110>
	B	{hkl}<110> … {112}
Components	C	{001}<110>
	D	{112}<111>
	E	{011}<111>
	F	{110}<001>

FCC vs. BCC {100} Pole figures

Table 1. Notation and Miller indices used for the different ideal orientations

A	$\{1\bar{1}1\}\langle 110\rangle$	C	$\{001\}\langle 110\rangle$
$\bar{A}$	$\{\bar{1}1\bar{1}\}\langle\bar{1}\bar{1}0\rangle$	D_1	$\{1\bar{2}1\}\langle 111\rangle$
A_1^*	$\{\bar{1}\bar{1}1\}\langle 112\rangle$	D_2	$\{\bar{1}\bar{1}2\}\langle 111\rangle$
A_2^*	$\{11\bar{1}\}\langle 112\rangle$	E	$\{0\bar{1}1\}\langle 111\rangle$
B	$\{1\bar{1}2\}\langle 110\rangle$	$\bar{E}$	$\{01\bar{1}\}\langle\bar{1}\bar{1}\bar{1}\rangle$
$\bar{B}$	$\{\bar{1}1\bar{2}\}\langle\bar{1}\bar{1}0\rangle$	F^*	$\{110\}\langle 001\rangle$

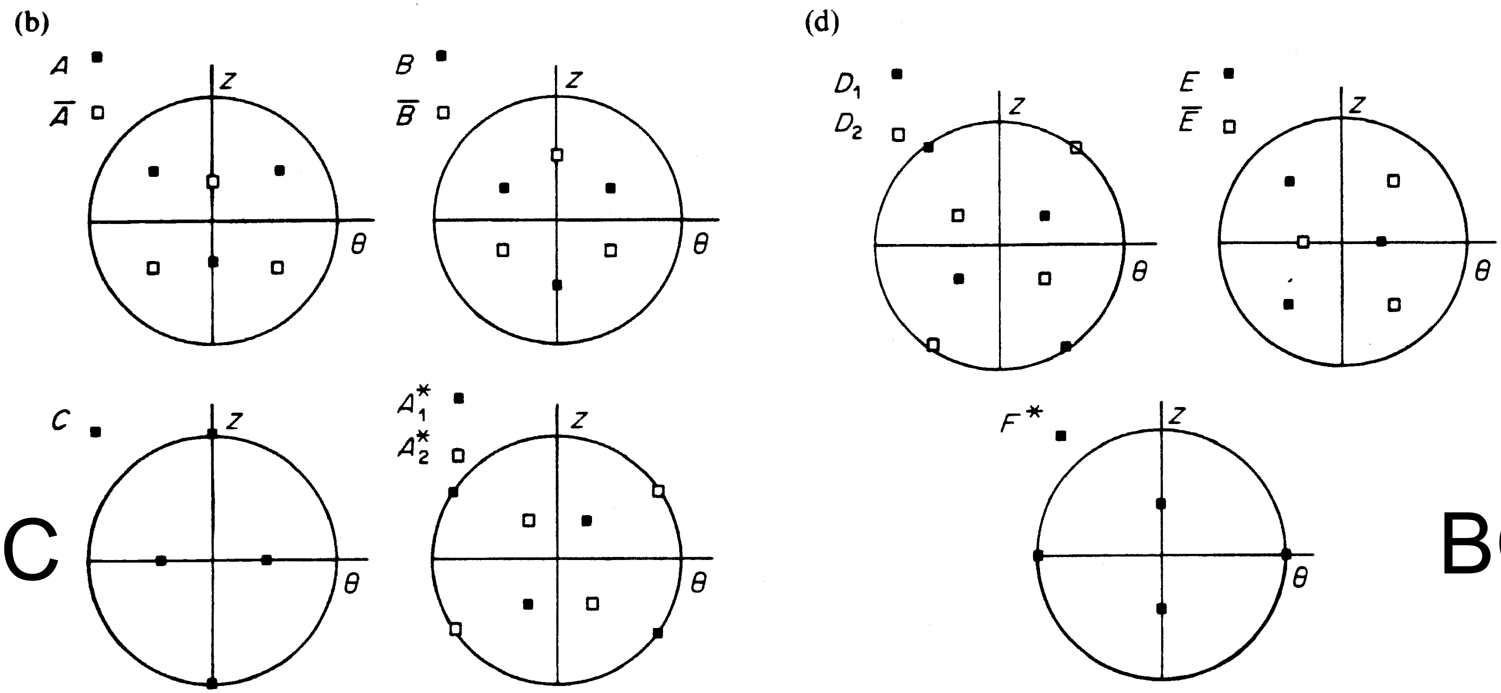

FCC

BCC

Fig. 4. Stereographic plots of the ideal orientations listed in Table 1. (a) and (c): inverse pole figures showing the orientations of the **j** and **k** unit vectors for the f.c.c. (a) and b.c.c. (c) components. The angle ψ is defined in Section 5. When $\phi = 0$, **j** and **k** coincide with the θ and z axes of the specimen, respectively. (b) and (d): {100} pole figures associated with the f.c.c. (b) and b.c.c. (d) ideal orientations.

Montheillet *et al*. (1985), *Acta metall*., **33** 705

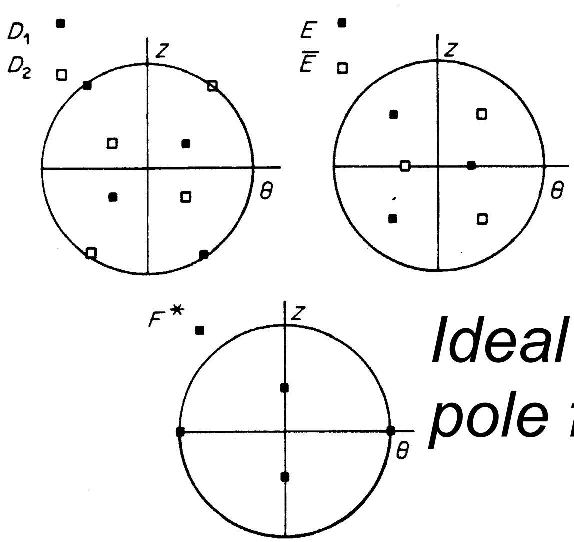

BCC torsion textures: Fe

Ideal |{100} pole figures

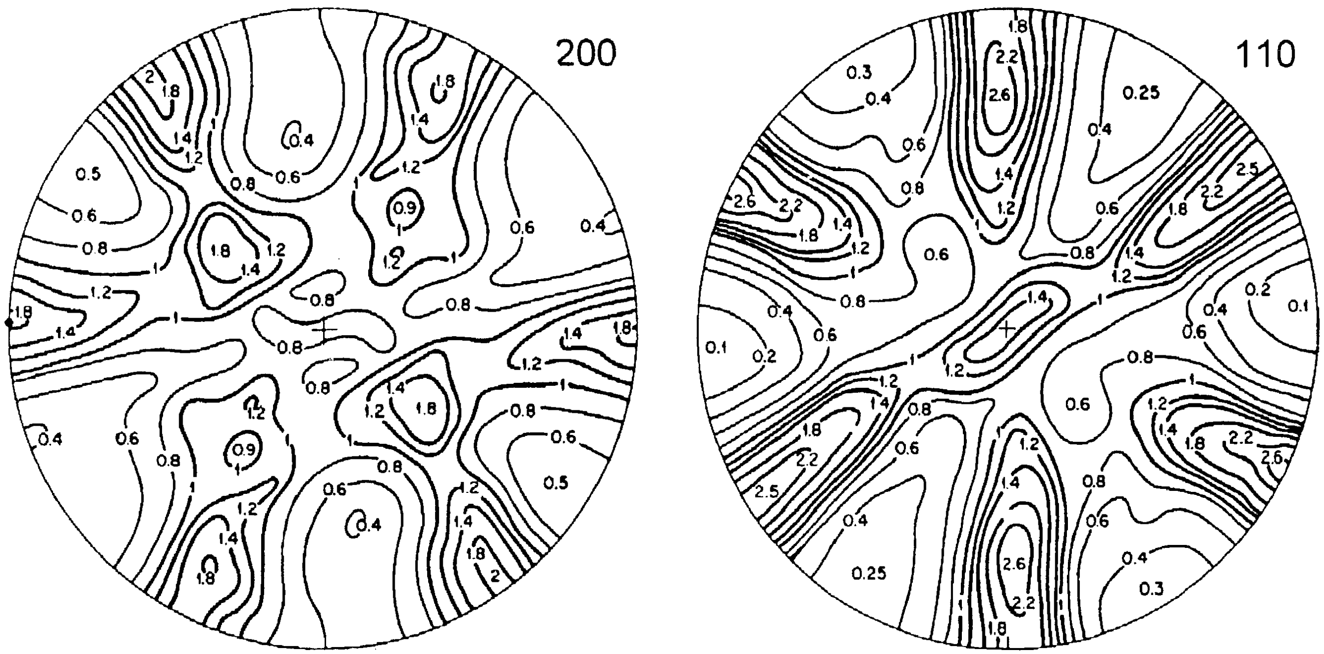

Fig. 18. Experimental 200 and 110 pole figures for Armco iron sheared to γ=2.1 (ε_{vM}=1.2) [WILLIAMS 1962] (Stereographic projection.) The shear direction points right on top.

BCC torsion textures: Ta

(a) initial texture from swaged rod;
(b) torsion texture

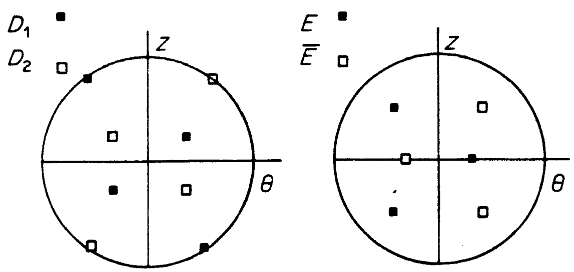

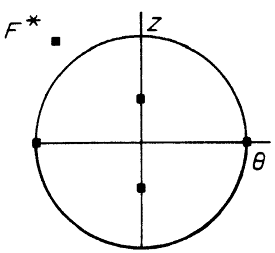

Ideal |{100} pole figures

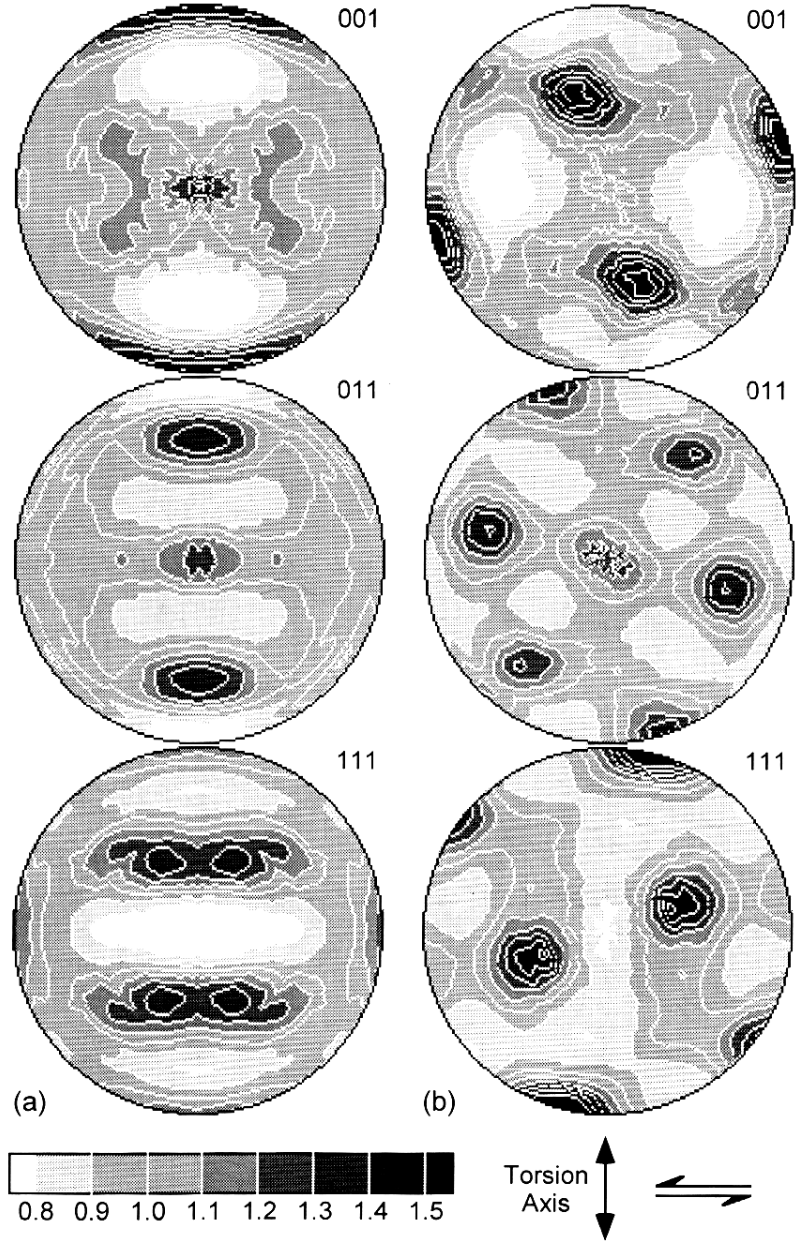

Fig. 19. Recalculated 111, 100 and 110 pole figures for tantalum: (a) initial texture; (b) tested in torsion to ε_{vM}=1.4. Equal-area projection.

Kocks, Ch. 5

Hexagonal Metals

- Common to show the (0001) pole figure: provides most information needed.
- Easy slip on the basal plane means that compression generally aligns the basal plane normal with the compression axis.
- Tension typically aligns basal plane normals perpendicular to the axis.

Deformation systems, hexagonal

TOMÉ *et al.*: MECHANICAL RESPONSE OF Zr. Part I

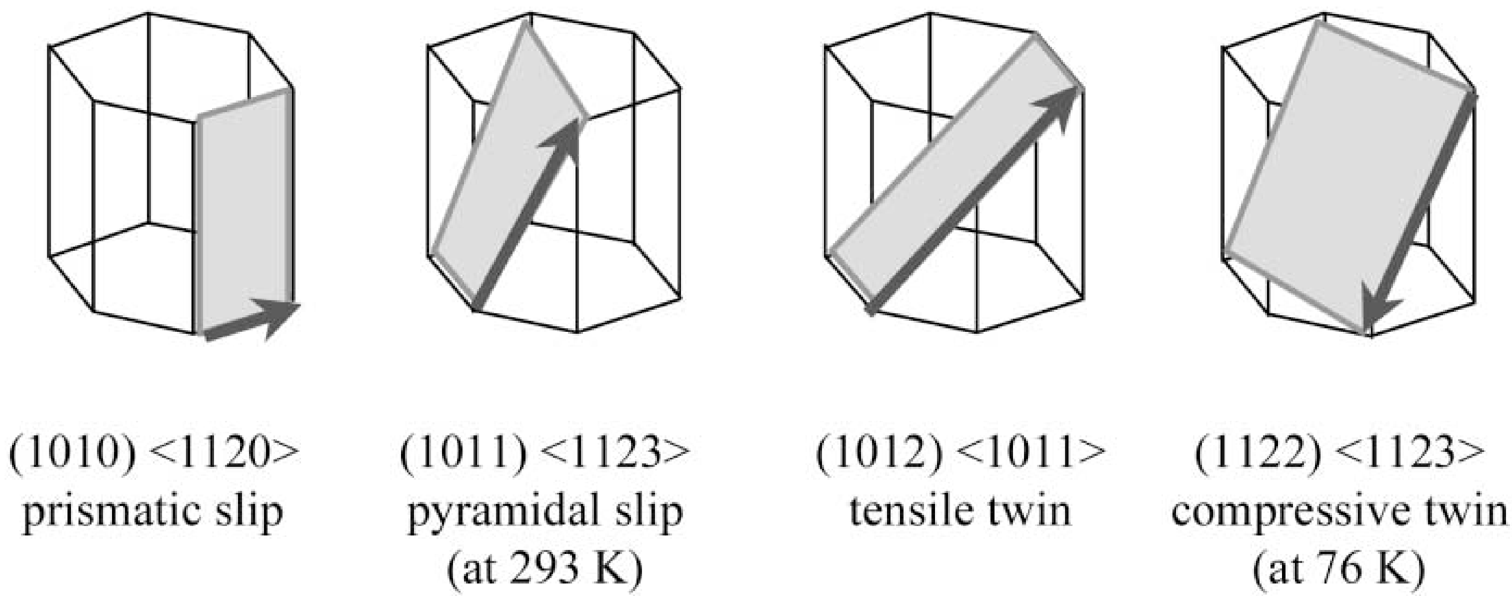

4. Active deformation systems in Zr considered in this work: prismatic slip, tensile twinning and py slip at 293K; prismatic slip, tensile twinning and compressive twinning at 76K.

Acta mater. **49** (2001) 3085–3096

Uniaxial textures in Ti

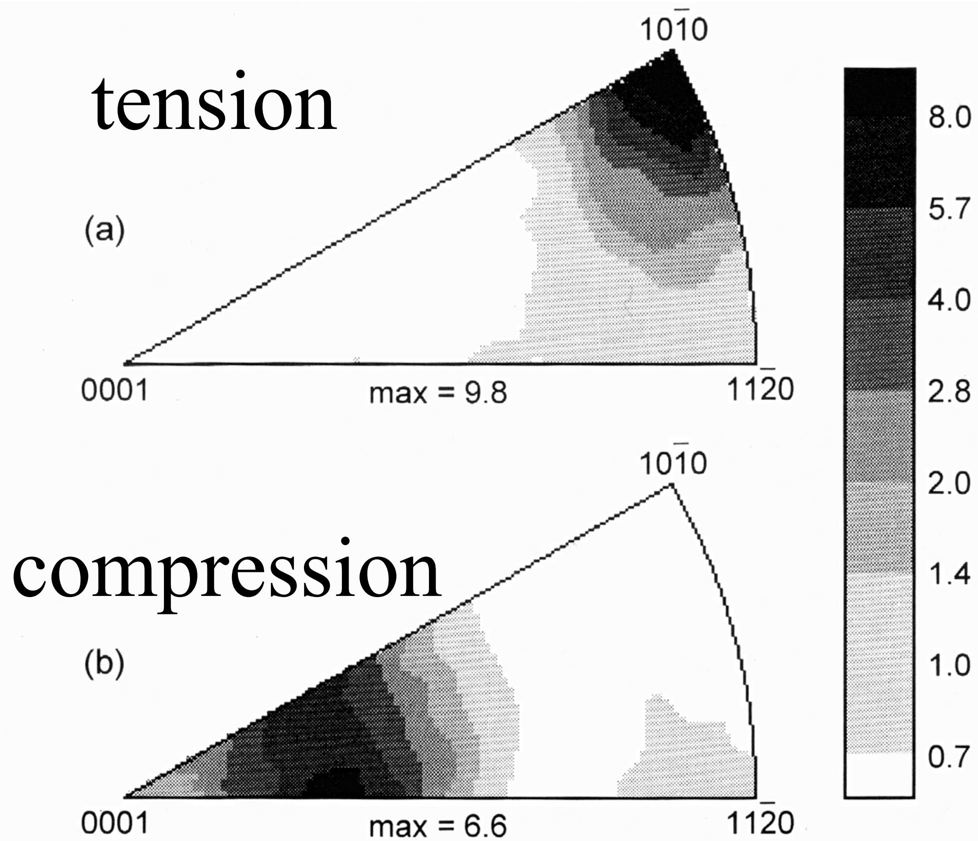

Fig. 20. Inverse pole figures of pure titanium: (a) extruded to a von Mises equivalent strain of 1.75 (extrusion-axis inverse pole figure), (b) forged and cross-rolled to a von Mises equivalent strain of 1.98 (plate normal inverse pole figure).

Compression: 25° from 0001, ~ <11-24>

Kocks, Ch. 5

Zr: compression

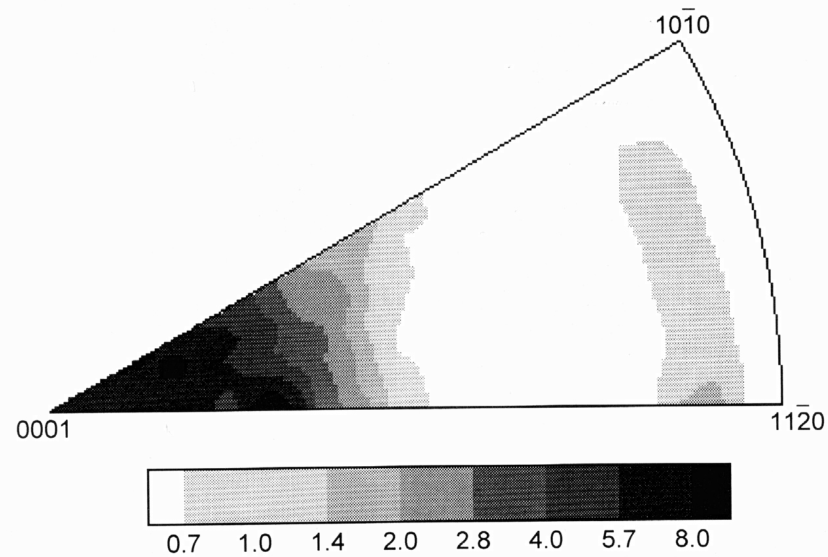

Fig. 21. Inverse pole figure (plate normals) for forged and cross-rolled zirconium, showing fiber texture near 0001.

Ti: compression

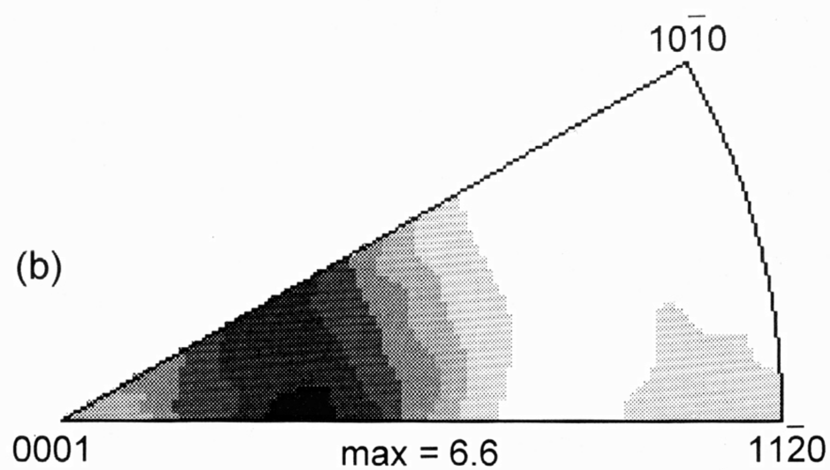

Kocks, Ch. 5

Hexagonal Rolling Textures; schematic

c/a > 1.633:
RD split in 0001

c/a < 1.633:
TD split in 0001

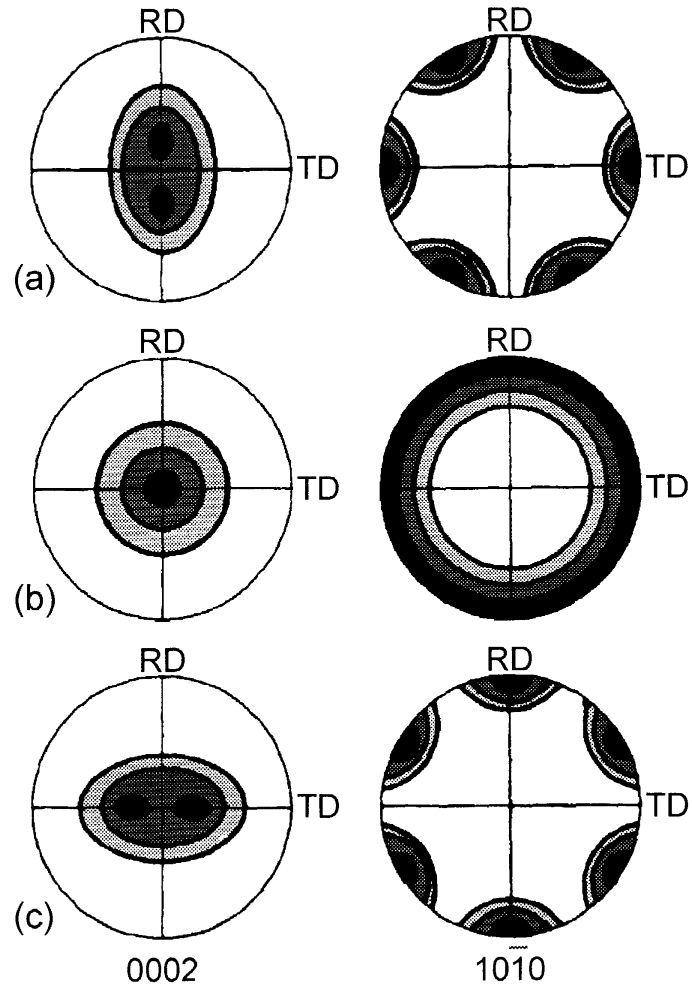

Fig. 22. Schematic rolling textures in hcp metals with *c/a* ratios of (a) greater than 1.633, (b) approximately equal to 1.633 and (c) less than 1.633. 0002 and 10$\bar{1}$0 pole figures. [TENCKHOFF 1988].

Kocks, Ch. 5

Hexagonal Rolling Textures: exptl.

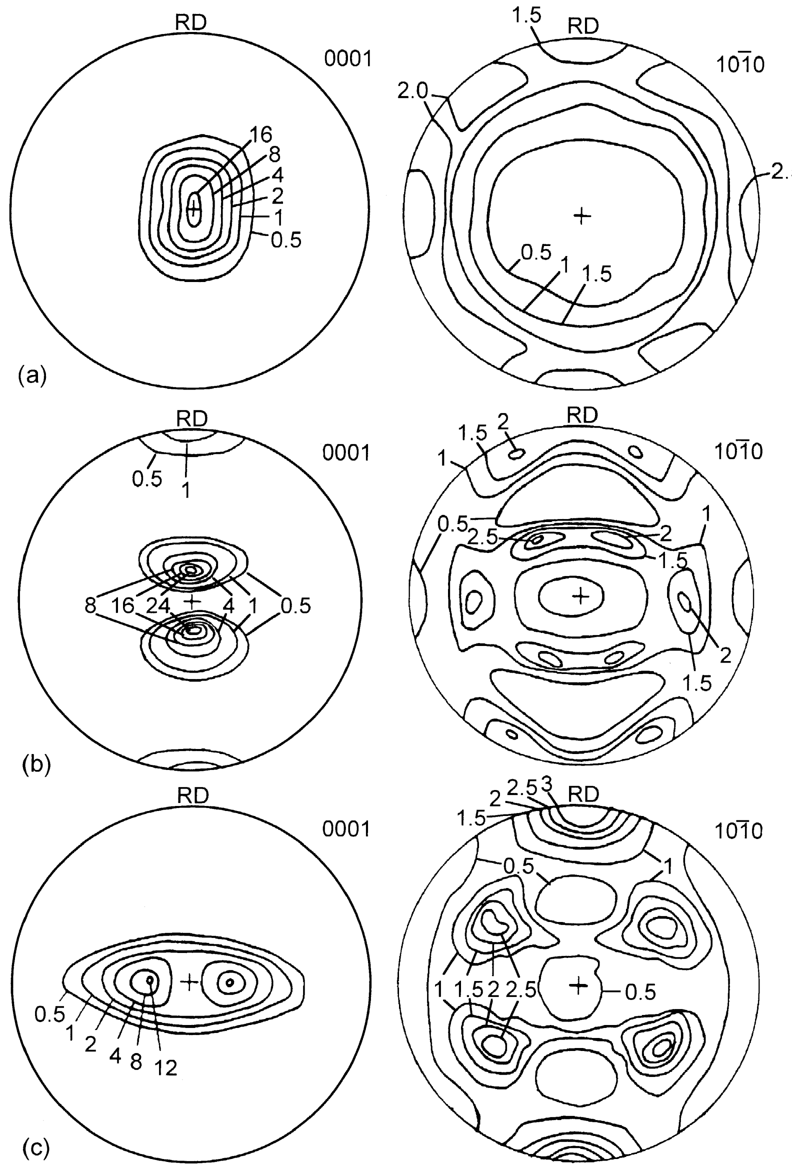

Fig. 23. 0002 pole figures for rolled (a) magnesium, (b) zinc, and (c) titanium, showing ⟨0001⟩ fiber for Mg, RD split for Zn, and TD split for Ti [GREWEN 1973] (stereographic projection).

Kocks, Ch. 5

Hexagonal Rolling: strain dependence

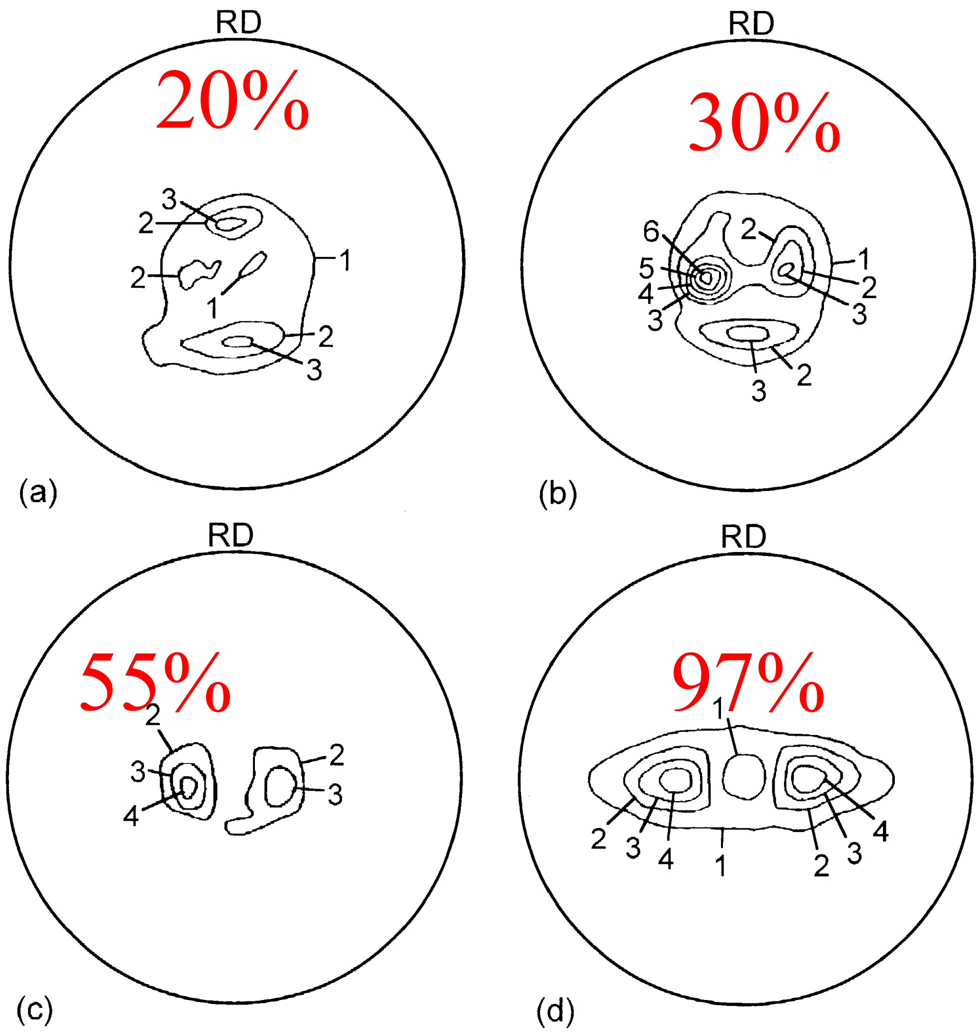

Fig. 24. 0002 pole figures for α-Ti sheet cold–rolled to thickness reductions of (a) 20%, (b) 30%, (c) 55% and (d) 97%. [BLICHARSKI &AL. 1979]. Stereographic projection.

Kocks, Ch. 5

Hexagonal: clock rolling

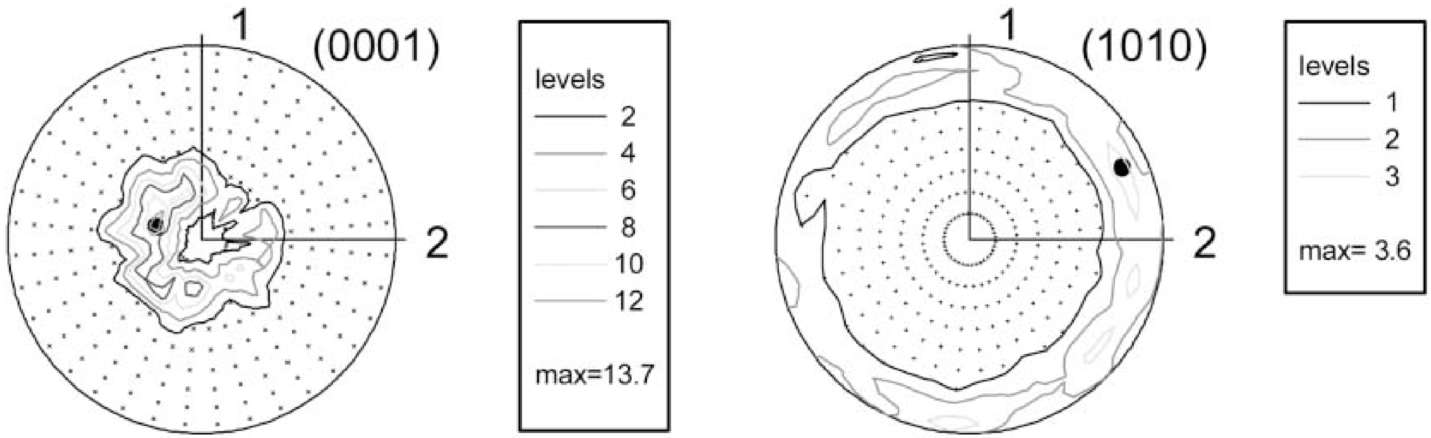

Fig. 1. Initial texture (basal and prism pole figures) of clock rolled Zr used in this study. Direction 3 coincides with the plate normal (ND).

Note the strong anisotropy caused by texture

Tomé *et al*. (2001)
Acta mater. **49**
3085–3096

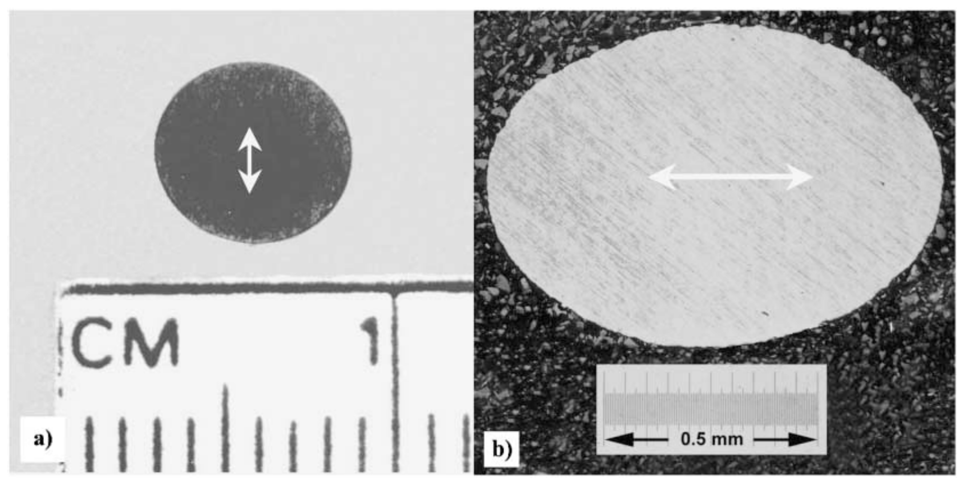

Fig. 3. Cross-section at the midpoint of high-purity zirconium samples deformed at LNT (76K) along the in-plane direction. (a) Deformed in compression (IPC) to 24% true strain; (b) deformed in tension (IPT) to 25% true strain. Double-ended arrows indicate the initial orientation of the basal poles.